

# Modeling of a Microbial Fuel Cell

**Michael Alexander Calder**

Master of Science in Energy and Environment

Submission date: August 2007

Supervisor: Johan Einar Hustad, EPT

Co-supervisor: Professor Paul D. Ronney, University of Southern  
California, USA



# Problem Description

Microbial Fuel Cells (MFCs) utilize bacteria to break down organic compounds in order to produce electricity. Much effort has been spent engineering conventional fuel cells (CFCs), but relatively little effort has been devoted to MFCs. Probably the most frequently used bacterium MFCs is *Shewanella Oneidensis*, which is metabolically incredibly versatile, being able to feed on a diversity of organic compounds and with certain metal oxides as their oxidant, thereby attaining energy for growth and survival. Properly harnessed, electrons released when the bacterial colony breaks down the compounds can be guided through electrodes and thereby produce usable electricity. This system is very similar to a CFC, using a Proton Exchange Membrane (PEM) to separate the anode and cathode sides, where the anode and cathode themselves are made of graphite felt. The bacteria act as an anode catalyst in the system, and platinum can be used conventionally as a cathode catalyst.

Development of a model of MFCs is not a simple extension of models of CFCs because of the many differences between MFCs and CFCs. These differences include much lower anode (fuelside) activity (expressed, for example, in term of current density); life-support and health requirements of the anode "catalyst" (bacteria); variability and adaptation (both desirable and undesirable) of the anode catalyst; and fuel (nutrient) complexity and flexibility. Despite these differences, we believe reaction-diffusion modeling, typically employed in chemical systems such as CFCs and combustion, will be a valuable tool for MFC engineering. Furthermore, because of the differences between MFCs and CFCs, it is considered very likely that viable MFCs will require novel architectures not employed in any CFCs.

Research aim for the master thesis:

- \* Construct a computational model simulating the key physical and chemical processes occurring in the MFC
- \* Start with a 1 -D model, and subsequently establish a 2-D model
- \* Model finned-membrane designs to enhance the power production

Research methodology

- \* Literature study
- \* Learn how to use GAMBIT (computational mesh generator), FLUENT (computational fluid dynamics software package) and possibly DetChem (FLUENT add-on for surface chemistry)
- Determine key variables influencing fuel cell power production
- \* Establish governing equations for each component of the MFC
- \* Make a simple 1-D model of the MFC
- \* Test simple model with empirical data, and if needed incorporate additional variables/factors
- \* Establish a 2-D model

Expected outcomes:

- \* Computational model of MFCs in FLUENT, 1D and 2D



## ***Preface***

The work presented in this Master Thesis was conducted at the University of Southern California (USC)'s Department of Aerospace and Mechanical Engineering, during Spring 2007. The thesis has been written during the 10<sup>th</sup> semester, and is prepared towards the fulfillment of my Masters Degree in Energy and Process Engineering studies at NTNU in Trondheim. The thesis has 130 pages, and was delivered August 10<sup>th</sup> 2007.

I would like to thank my fellow students at USC both for ideas towards the thesis, and for experimental data that I needed for my computational model. I would like to thank my Norwegian coordinator Johan Hustad for helping me making it possible to perform my thesis research abroad.

Finally, I would like to thank Professor Paul Ronney for all his tips, guidance and inspiration that he has given me while I have been at USC.

---

**Michael A. Calder**

## **Abstract**

It is clear that society worldwide must immediately begin to mitigate its environmental damage in order to sustain life on Earth. In this regard, researchers all over the globe are exploring new energy efficient alternatives to power everything from cars to cell phones. The following brief describes research conducted on Microbial Fuel Cells (MFC) and its ability to utilize bacteria to produce electricity from biological masses for low energy consumer products. While structurally the MFC is very similar to a Conventional Fuel Cell, the two systems have inherent differences that change the reactions, inputs and energy output. Currently, we have found MFC to produce only a fraction of the power ( $\sim 1\text{A}/\text{cm}^2$  vs  $\sim 1\text{mA}/\text{cm}^2$ ) produced by a conventional CFC, however, its versatility keeps MFCs as a promising fuel source potential.

A Multi-disciplinary University Research Initiative has organized to examine and test the potential of MFC. The team is divided into three teams based on industry domains and expertise: microbiology, chemistry and electrochemistry, and engineering and modeling. The following master thesis research was part of the engineering and modeling team lead by Professor Ronney XX. The goal of our team was to construct a first version of a computational model simulating the MFC system. The computational model is based on combustion kinetics and a diffusion-reaction system theories, and is manipulated to imitate a biological system that can maximize its energy output.

The model has been constructed in Fluent. Starting out with a 1D model, and consequently moved on to a 2D version. The final model is a diffusion-reaction system with 6 different species, a 3-step reaction, including a bacterial anodic oxidation, a cathodic reduction, and a possibility of taking into account a counteracting anodic reaction for oxygen crossover through the membrane. While the model has been proven to correlate well with lab tested experimental results, the team will continue to identify conditions to maximize the MFC's efficiency and energy output.

## **Table of Contents**

<b>1</b>	<b>Introduction</b> .....	<b>2</b>
1.1	Background .....	2
1.2	Multi-disciplinary University Research Initiative .....	2
1.3	Scope of the Present Study .....	3
<b>2</b>	<b>Microbial Fuel Cell Technology &amp; Model Approach</b> .....	<b>4</b>
2.1	How Does a Conventional Fuel Cell work? .....	4
2.2	How does a Microbial Fuel Cell work? .....	6
2.3	MR1 – <i>Shewanella oneidensis</i> .....	9
2.4	Modeling Approach .....	10
2.5	Basic Assumptions.....	12
<b>3</b>	<b>Empirical Data</b> .....	<b>13</b>
3.1	The system being modeled.....	13
3.2	Experiment Case 1 .....	16
3.2.1	Experiment #1 .....	16
3.2.2	Experiment #2.....	17
3.2.3	Experiment #3.....	18
3.3	Experiment Case 2 .....	20
<b>4</b>	<b>Governing Equations for MFC FLUENT model</b> .....	<b>22</b>
4.1	Species Calculations in FLUENT .....	22
4.2	Species and Charge Transportation .....	24
4.2.1	Species Transportation in FLUENT .....	25
4.2.2	Charge Transfer .....	27
4.3	Reaction Equations .....	27
4.3.1	Volumetric Reactions.....	28
4.3.2	Surface Reactions.....	30
	Electrical Model.....	32
4.4	Membrane .....	35
<b>5</b>	<b>Selecting Appropriate Models and Values</b> .....	<b>36</b>
5.1	Dimensions .....	36
5.2	Species and Reaction Mechanisms .....	37
5.2.1	Experimental Reactions vs. Modeling Reactions .....	38
5.2.2	Modeling Species.....	39
5.2.3	Reactions and Mechanisms.....	40
5.2.4	Reaction rates.....	42
5.2.5	Next generation reaction mechanisms .....	43
5.3	Concentrations .....	44
5.4	Diffusivities.....	50
5.4.1	Laminar Mass Diffusion Coefficients.....	50
5.4.2	Turbulent diffusion .....	52
5.5	Membrane .....	53
5.5.1	Porous Media .....	54
5.5.2	Diffusivity Reducing Media .....	54
5.6	Power Estimations .....	56

<b>6</b>	<b>Setting up and Running the MFC model in FLUENT .....</b>	<b>57</b>
6.1	Computer Lab .....	57
6.2	Geometry in GAMBIT .....	57
6.2.1	Geometry and Zones .....	57
6.2.2	Mesh.....	59
6.2.3	Zone Settings .....	60
6.2.4	Importing the mesh into FLUENT.....	61
6.3	Settings.....	61
6.3.1	Solver Settings .....	61
6.3.2	Boundary conditions .....	64
6.4	User Defined Functions .....	66
6.4.1	FLUENT and UDF .....	66
6.4.2	Applying Diffusivities by use of UDF.....	66
6.4.3	Future UDF possibilities .....	68
6.5	Running the Model .....	68
6.5.1	Iterations .....	68
6.5.2	Schemes .....	69
6.5.3	Storing.....	69
6.6	Excel Analysis .....	70
<b>7</b>	<b>Tests and Results from Computational MFC Model.....</b>	<b>71</b>
7.1	Finding Appropriate Reaction Rates.....	71
7.2	Varying oxygen concentrations .....	75
7.3	Turbulence .....	77
7.4	Oxygen crossover from cathode to anode.....	79
7.5	Diffusion Calculations .....	81
7.6	Geometries 2D .....	82
<b>8</b>	<b>Discussion.....</b>	<b>83</b>
<b>9</b>	<b>Conclusion .....</b>	<b>86</b>
<b>10</b>	<b>Bibliography .....</b>	<b>87</b>
<b>11</b>	<b>Appendices.....</b>	<b>90</b>



## List of Tables

Table 2.1 - CFC and MFC comparison.....	13
Table 3.1 - Specific Data from MFC Experiments.....	20
Table 3.2 - Carbon Balance for nutrient decomposition data .....	26
Table 4.1 - Transportation Processes Relevant to Fuel Cells .....	30
Table 5.1 - MFC Model Dimensions .....	42
Table 5.2 - Properties of Selected Modeling Species .....	45
Table 5.3 - Maximum Species Concentraions .....	54
Table 5.4 - Diffusivity Coefficients based on Approximated Relative Factors.....	55
Table 5.5 - U.S. EPA Laminar Diffusion Coefficients .....	56
Table 5.6 - Bubble Speed.....	58
Table 5.7 - Simulated Diffusion Coefficients of H <sup>+</sup> ions in a Nafion 117 membrane	60
Table 6.1 - Boundary conditions for MFC model.....	70
Table 6.2 - Interpreted UDF Diffusivity Settings .....	72
Table 6.3 - Compiled UDF Diffusivity Settings .....	73

## List of Figures

Figure 1.1 - Flow Diagram of MURI Teamwork .....	8
Figure 2.1 – Simple 2 Chamber PEM Fuel Cell .....	10
Figure 2.2 - Mediated or Mediator-Less MFC.....	11
Figure 2.3 - Picture of the actual MFC .....	12
Figure 2.4 - Graphite Felt and Shewanella .....	14
Figure 2.5 - Shewanella MR-1 Nano wires <sup>5</sup> .....	15
Figure 2.6 – Sketch of Lab Setup and Specific Modeling Zone .....	16
Figure 3.1 - Sketch of MFC .....	18
Figure 3.2 - Graphical Presentation of Voltage & Power vs. Current for an MFC .....	21
Figure 3.3 - Stirring Experiment .....	24
Figure 3.4 - Graphical Presentation of Various Species Concentration in MFC.....	26
Figure 6.1 - GAMBIT Layers .....	63
Figure 6.2 – GAMBIT MFC Model Wires .....	64
Figure 6.3 – GAMBIT MFC Model Meshing .....	65
Figure 6.4 – FLUENT Solver Menu .....	66
Figure 6.5 - FLUENT Species Model Menu .....	67
Figure 6.6 - FLUENT Materials Menu .....	67
Figure 6.8 a&b - FLUENT Reactions and Mechanisms .....	69
Figure 6.9 - FLUENT Iterations .....	74
Figure 7.1 a&b – Nutrient and Oxygen Concentrations, Anode reaction rate: 1e-6 ...	76
Figure 7.2 a&b - Nutrient and Oxygen Concentrations for Anode reaction rate: 1e-477	77
Figure 7.3 - Estimated Current for MFC - With oxygen limitation.....	78
Figure 7.4 - Finding required reaction rate .....	79
Figure 7.5 - Current Depending on Oxygen Concentration.....	80
Figure 7.6 - Current as a function of turbulence intensity in anode chamber.....	82
Figure 7.7 - Crossover effect of oxygen .....	85

## Nomenclature

$Y_i$  Mass fraction of species  $i$

$X_i$  Mole fraction of species  $i$

$C_i$  Molar concentration of species  $i$  in moles per  $m^3$

$M_{w,i}$  Molecular weight of species  $i$ , kg/ kmol

$M_{w,m}$  Molecular weight of mixture, kg/ kmol

$D$  Diffusivity,  $m^2/s$

# 1 Introduction

## 1.1 Background

Microbial Fuel Cells (MFCs) utilize bacteria to break down organic compounds in order to produce useful electricity. The *Shewanella oneidensis* MR-1 is the bacteria most frequently used because of its incredible ability to utilize different carbon sources and reduce a variety of electron acceptors. This allows the MFC to be highly flexible with regards to fuel requirements, and therefore allowing the use of many types of biomasses to power the cell.

By understanding the MFC system, it will be possible to optimize the properties and design of the fuel cell for maximum efficiency. It will also be possible to scale the system up or down for use in applications which could include pure power production purposes, waste disposal, remote power supplies, water treatments or other uses. The design of the cell can be optimized by testing various designs on a computational model and selecting the most promising solutions for lab testing. Since lab testing is time intensive and expensive, computational modeling allows for a cost effective way to assess all many solutions under different conditions. Once a sufficiently accurate model has been produced, new designs can be tested very quickly.

Developing a computational model of a MFC cannot just be a simple extension of the already existing fuel cell models designed for Conventional Fuel Cells (CFCs). Despite of the many similarities in the way the fuel cells operate work, there are clear distinct differences between them will require a new model to be developed. The differences and similarities between MFC and CFCs will be delineated in section 2.2.

## 1.2 Multi-disciplinary University Research Initiative

To fully understand the MFC you have to understand all the different aspects of the system. These aspects are unusually diverse including areas such as biological technology, bacteria metabolism, electrical circuits, reaction kinetics, and membrane technology. Therefore, this research is part of a Multidisciplinary University Research Initiative (MURI), funded by the *Air Force Office of Scientific Research*.

The research group is led by Professor Kenneth Nealson, the scientist who discovered the *Shewanella* bacteria in 1987, and is supported with a team of professors and student researchers, where a majority is from University of Southern California (USC). Specifically, the team consists of researchers from the 3 disciplines; microbiology, chemistry and electrochemistry, and engineering and modeling. As a result, an important part of the project has been meetings and presentations involving all participants in order to continually share information and ensure cohesion of the MFC. By combining experimental data with theoretical and computational models, new ideas have emerged and lead to improved modeling, integrated assumptions and ultimately higher power output and efficiency (see Figure 1.1). The long term goal for the 5 year MURI Microbial Fuel Cell project is to produce a self-propelled MFC on a simple robotic chassis<sup>1</sup>.

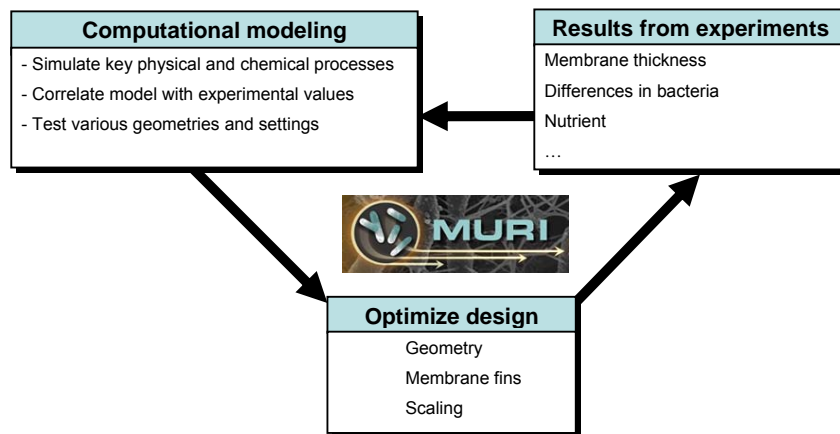


**Figure 1.1 - Flow Diagram of MURI Teamwork**

### **1.3 Scope of the Present Study**

The focus of this master thesis research is the engineering modeling of the MFC system, and is supervised by Professor Paul Ronney at the Aerospace and Mechanical Engineering department at USC. The scope of the thesis includes constructing a computational model to simulate the key physical and chemical processes occurring in the MFC. Starting with a 1-D model, and subsequently establishing a 2-D model, that will correspond to the experimental microbial fuel cell results from the extended research group.

## 2 Microbial Fuel Cell Technology & Model Approach

### 2.1 How Does a Conventional Fuel Cell work?

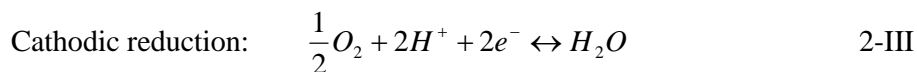
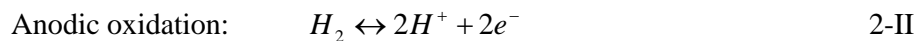
The purpose of a fuel cell is to create useful electrical power from a fuel by electrochemical conversion, rather than having to burn the fuel, which is the method used if electricity is to be produced with a combustion engine. When using traditional thermal engines for electricity production there is always a large heat loss, which decreases the efficiency drastically. In addition, combustion driven engines can reach very high temperatures, which can be hazardous in certain situations.

Most Conventional Fuel Cells (CFC) utilizes either hydrogen (H<sub>2</sub>) or other high grade hydrocarbons (methanol, etc) as fuels, and normally uses oxygen from the air as oxidizer. In order to explain how the fuel cell works, a very simple chemical reaction will be investigated on a molecular scale:



In this reaction, the hydrogen-hydrogen (H-H) bond and oxygen-oxygen (O-O) bonds are broken, and new hydrogen-oxygen (H-O-H) bonds are created. The energy of the H-O-H bond configuration is lower than the bond for the reactants (O-O and H-H), and therefore energy is being released. The explanation on a molecular scale is that the electrons change configuration from one bond state to another. However, since this occurs on a nano timescale, the only energy conversion possible is turning the energy into heat.

If the timescale of the reaction can be increased, it makes it easier to control the energy release. A fuel cell makes use of a physical separation to divide the global reaction into two separate partial reactions. The first reaction is an oxidation reaction, which splits up the H<sub>2</sub> into H<sup>+</sup> ions and electrons (see equation XX). The second reaction is a reduction reaction, where the H<sup>+</sup> ions combine with oxygen and electrons to produce water (see equation XX). By separating the reactions, it is possible to gain control over how the electrons are transferred.



One of the simplest fuel cells possible consists of only one chamber with a liquid electrolyte, two electrodes and reactants being supplied locally at each electrode. The function of the electrolyte is to allow transportation of  $H^+$  ions, while limiting the transport of electrons. Because of the energy difference in the electron bond configuration, it is possible to make it advantageous for the electrons to go from the anode electrode, through an electrical circuit, in order to react at the cathode electrode and help form water.

For higher efficiency, the anode and cathode can be separated into two different chambers by a Proton Exchange Membrane (PEM), as seen in Figure 2.1. This allows for a higher reactant concentration without causing a crossover of reactants, and thereby increases the power production.

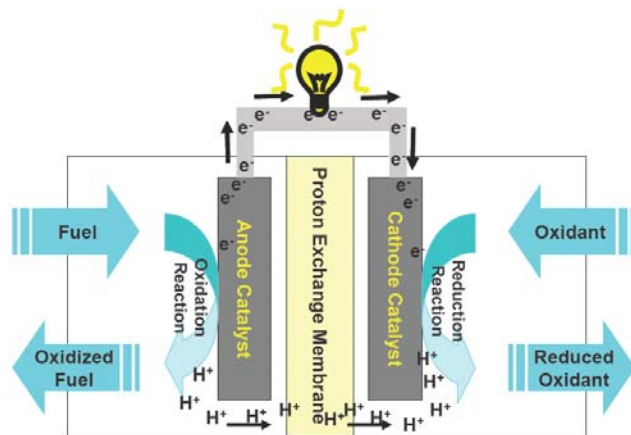


**Figure 2.1 – Simple 2 Chamber PEM Fuel Cell<sup>2</sup>**

In order to attain a voltage and current high enough to be convenient to use, fuel cells are connected and packed together in close bunks. The CFC technology is constantly improving, which means they can be made increasingly more compact and efficient. The CFC has already started to take up the fight on the electronics market, where instead of becoming gradually depleted like a battery, a fuel cell produces electricity as long as it has a supply of fuel and oxidizer. And since hydrocarbons are far more compact than lithium batteries, a laptop could run for many days on a small tank.

## 2.2 How does a Microbial Fuel Cell work?

The components of a MFC are very similar to the ones of the CFC. It has two chambers divided by a membrane, with one electrode in each chamber. Fuel is supplied on the anode side where an oxidation reaction produces electrons and  $H^+$  ions, while an oxidizer is supplied on the cathode side resulting in a reduction reaction. But, when going into deeper details, the differences become clear (see Table 2.19).

Overall, the two main differences arise from the type of catalyst and the energy source used. The CFC uses expensive materials such as platinum to act as a catalyst, whilst the MFC uses bacteria to promote and increase the reaction rate in the anode reaction. And instead of using hydrogen ( $H_2$ ) or other high grade hydrocarbons as fuel, the MFC uses various biological materials as its nutrient and energy source.

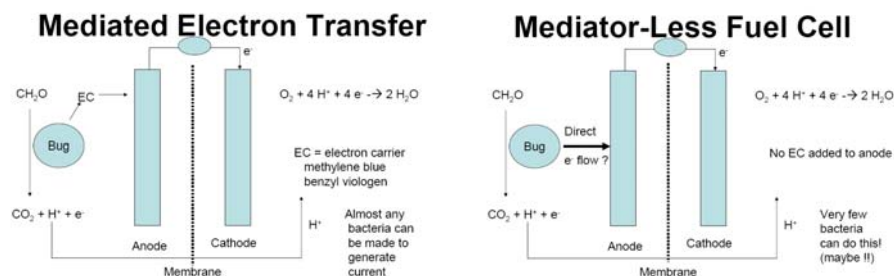


Figure 2.2 - Mediated or Mediator-Less MFC

MFCs can be either mediated or mediator-less (see Figure 2.2). In mediated fuel cells, bacteria are suspended in the anode solution together with the nutrient, and because of some sort of electron carrier that is added to the liquid in the anode chamber, the electrons can be transported from the bacteria through the liquid to the electrode. Almost any type of bacteria can be used in this type of MFC, but a lot of electrons and energy is however lost in the process, which limits the total efficiency of the fuel cell drastically. Mediator-less fuel cells however, are fuel cells that does not require any additional electron carrier in the solution in order to transport electrons from the bacteria to the electrode. This process gives better control over the fuel cell and allows for a higher efficiency potential. However, they do require very special



bacteria. The MFC that is being modeled in this master thesis research is a mediator-less fuel cell, and it uses the bacteria *Shewanella oneidensis* MR1 (section 2.3).

The MR-1 can break down a broad range of different biological material, and if it is harnessed in the correct way, and prevented from breathing oxygen, it will emit  $H^+$  ions and electrons while doing it. If used in a fuel cell, the  $H^+$  ions pass through the membrane (PEM) into the cathode chamber, whilst the electrons are forced to go through the electrical circuit in order to get to the cathode electrode. At the cathode electrode the species react together with oxygen and creates water ( $H_2O$ ), much like a CFC. For a more detailed description on the MFC that has been used for the modeling, see section 3.1 and Figure 2.3.

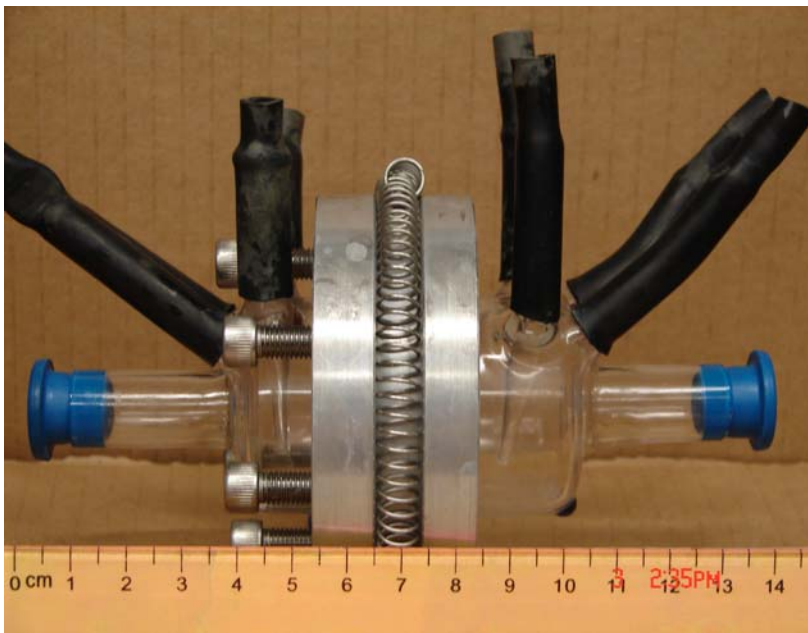


**Figure 2.3 - Picture of the actual MFC**

The MFC has many possible advantages over CFC, which is one of the reasons an increasing amount of research is being conducted on it. First of all, the catalyst for the MFC is essentially free, since the bacteria can be grown almost anywhere. Whilst in a CFC, the catalyst is responsible for a substantial part of the total cost. The bacteria are also versatile, so that the same MFC can be used with many different types of fuel. In addition, the bacteria has been tested and found to be very robust, which means it can survive under extreme conditions of pH, temperature and salinity.

And since the catalyst is produced by live cells, it can even have the ability to repair and heal itself if it is allowed. There are around 50 types of *Shewanella* species known, and all that are tested have shown to produce current if used in a MFC. It is believed that a lot of improvement can be done not only by changing the design of the fuel cell, but also by using microbiology to construct the best possible bacteria.

However, the present MFC tests also show some disadvantages. The most obvious disadvantage is the low current density that has been achieved. Whilst CFC can obtain current densities in the order of  $1 \text{ A/cm}^2$ , the current MFC experiments has only showed around  $1 \text{ mA/cm}^2$ . It is believed that this can be increased by further developing the design of both the fuel cell and the bacteria itself. However, even if it may have trouble reaching up to the same high power density as CFCs, its other advantages may still allow it a place in the market. Other problems that have occurred in the MFC shows that it has been difficult to keep the fuel cell running without the requirement of maintenance, and that it has been more sensitive to breakdown and decay than what would be preferable if it is to be used in a commercial system.

**Table 2.1 - CFC and MFC comparison**

Description	Conventional Fuel Cell	Microbial Fuel Cell
<b>Fuel</b>	Hydrogen (H <sub>2</sub> )	Lactate or other biological mass
<b>Waste/ Exhaust</b>	H <sub>2</sub> O	H <sub>2</sub> O and partially decomposed nutrition / fuel
<b>Anode Catalyst</b>	Typically platinum Expensive material	<i>Shewanella oneidensis</i> MR-1 (Micro-organisms) Inexpensive to produce
<b>Reaction Mechanisms</b>	Combustion kinetics	Live biological system
<b>Current density</b>	$\sim 1 \text{ A/cm}^2$	$\sim 1 \text{ mA/cm}^2$

### 2.3 MR1 – *Shewanella oneidensis*

The *Shewanella oneidensis* MR-1 was discovered and first isolated in 1988 by Dr. Kenneth Nealson from sediments of Lake Oneida in New York<sup>3</sup>, and is probably the most frequently used bacteria in MFCs. The MR-1 is famous for its ability to reduce solid substrates (Fe and Mn oxides), it can grow both aerobically and anaerobically, growing quickly on defined mediums (see Figure 2.4)<sup>4</sup>.

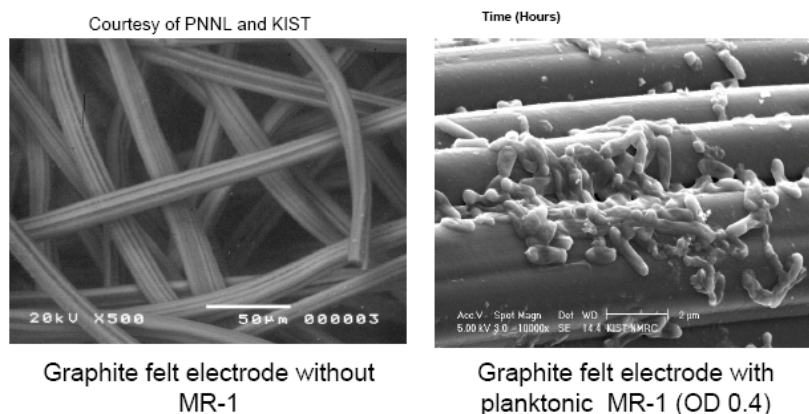


**Figure 2.4 - Graphite Felt and *Shewanella***<sup>5</sup>

It usually uses oxygen as its electron acceptor for biological species in order to remove a surplus of electrons. However, if there is no oxygen available, the MR-1 bacteria have an amazing ability to use various metals as electron acceptor in order to survive. It is not completely understood how this is done, but it is believed that by growing on the electrode surface, the bacteria can use the electrode to breathe through direct contact. Additionally, microscope pictures have shown that some type of nano wires<sup>6</sup>, which have proved to be electrically conducting<sup>7</sup>, are produced between MR-1 cells. This might allow also bacteria that are not in direct contact with the electrode to emit electrons.



**Figure 2.5 - Shewanella MR-1 Nano wires<sup>5</sup>**

From the large variety of different strands of Shewanella that have been isolated, MR-1 was chosen for use in the main tests of the MURI MFC project. Tests are also being performed on the other strands in order to see if there are any that will work more efficiently or have differing properties that can be beneficial for the MFCs.

## ***2.4 Modeling Approach***

A vast amount of research has been performed on CFCs, which over time has made it a well understood technology. By utilizing various methods<sup>8</sup> to model CFCs and optimize its design and use, it is now possible to make them very compact and efficient. To understand the MFC system better, a good starting point is to compare it with the already well known CFC theory. However, it is not just a simple extension of the CFC model, and it is important to be aware of the differences between the systems. These differences are believed to be a much lower anode (fuel-side) activity (expressed, for example, in terms of current density); life-support and health requirements of the anode "catalyst" (bacteria); variability and adaptation (both desirable and undesirable) of the anode catalyst; and fuel (nutrient) complexity and flexibility.

The modeling strategy has been to use a dynamic model. In stead of implementing all possible variables in the model at once, it started out as simple model with only 2 species and diffusion. By increasing its complicity gradually it became more and more accurate, taking into account an increasing amount of factors. Even though the MFC is a biological system, compared to the purely chemical systems that are found

in CFC and combustion, it was thought that similar reaction-diffusion type modeling used in these chemical systems would prove to be valuable tools. The experimental tests from Case 1 (details in section 3.2) will be used as a base for the initial model. Figure 2.6 shows the specific area of the MFC that will be modeled.

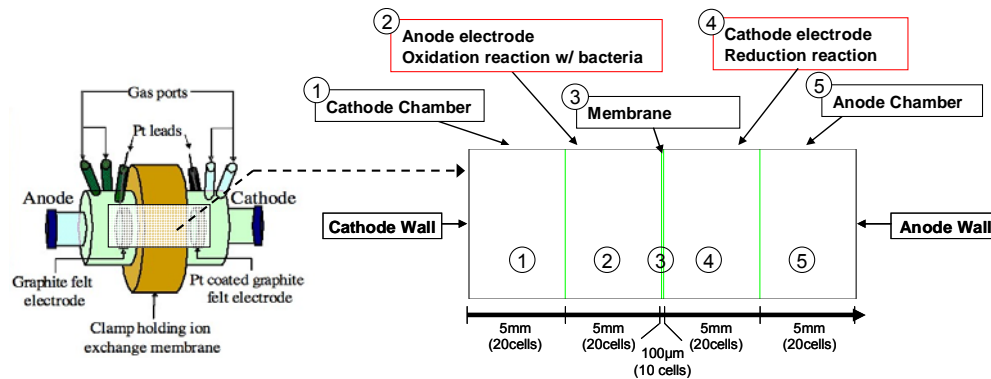


**Figure 2.6 – Sketch of Lab Setup and Specific Modeling Zone**

FLUENT<sup>9</sup> Computational Fluid Dynamics (CFD) program has been selected to model the system. The program allows the user to import a geometric mesh, and then manually change flow patterns, boundary conditions, reaction kinetics, and most importantly also allow altering all possible variables in the system with customized User Defined Functions (UDF). The digital mesh can be constructed in various mesh generating programs, though the researcher decided to use GAMBIT, which is the suggested program that is delivered with the FLUENT software.

Performing reality checks on the FLUENT results has had a high priority and have been carried out parallel to making new versions of the model. In general, all computer programs are ruled by GIGO (Garbage In – Garbage Out). If a computer program is given faulty or incomplete input, it will give back faulty or incomplete results. FLUENT is no better in this respect, and it is therefore very important to carry out regular reality checks in order to check whether the model is working correctly. A selection of the reality checks performed can be found in Appendix.

The computational model will be based on results from various experimental lab tests performed on MFCs. Additional values that can not be found from these experiments will be found from literature. The goal is to make a model that correlates to existing

data, in such a way that it can be used to predict new results. The initial factors that will be taken into account are transportation of various species, reaction between species, electrodes and bacteria, and the electrical current that is achieved by the MFC.

## **2.5 Basic Assumptions**

When constructing the MFC model, it is assumed that the anodic reaction rate or bacteria activity is the limiting factor in the fuel cell. Therefore the focus will be on held on the anode side, with fewer restraints on the cathode electrode. As with all fuel cells, it is assumed that the surface area of the membrane/electrode area is proportional to the MFC effect, in such a way that a doubling of surface area induces a doubling of the MFC effect. Modeling results and experimental results will therefore be calculated and compared in a per projected area unit.

It will also be assumed that the MFC working in steady state has the same current, voltage and power properties as of the max values from the batch mode results.

### 3 Empirical Data

A wide selection of empirical data has been made available through the MURI network for use in the initial computational model. Most of the experimental data that has been used has come from two different groups in the network, both located at the University of Southern California. The significant results from these experiments will be presented and discussed with respect to important values for the model.

The fuel cell that the experiments have been conducted on will also be presented, since it has been used as a base for the computational model.

#### 3.1 The system being modeled

The type of fuel cell that will be modeled is a mediator-less fuel cell (section 2.2), with anode and cathode being separated by a Nafion 117 membrane (see Figure 3.1). The electrodes on both anode and cathode side were made of carbon felt, and platinum had been added to the cathode electrode as a catalyst, lowering the cathodic activation energy. The setup is simple and allows for easy control and manipulation of the important variables, whilst minimizing the uncontrolled variables.

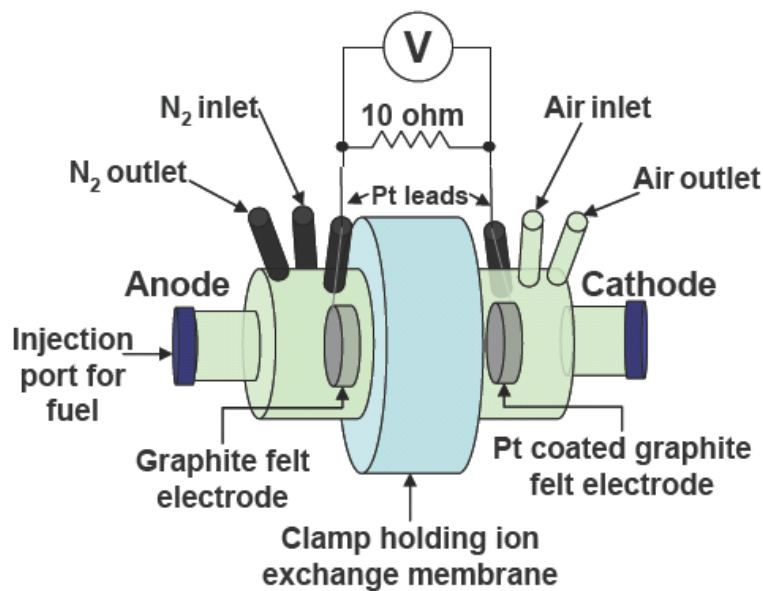


Figure 3.1 - Sketch of MFC

Lactate acted as a fuel and nutrient to the bacteria. Lactate is a solution of lactic acid ( $C_3H_6O_3$ ), which forms lactate ion  $C_3H_5O_3^-$  and  $H^+$ . Batch feeding was used in the experiments, which meant that instead of having a continuous flow of reactants as in a normal CFC, a specific amount of nutrient was injected into the anode chamber at given time intervals. This gave the fuel cell a periodic oscillation in the voltage, current and power production. Ideally, the MFC should be run with a continuous flow of nutrient, which would allow for a more stable power production.

The second reactant needed in the MFC process is oxygen, which was attained by bubbling air into the cathode chamber. It is assumed that if air is bubbled into the chamber at a high enough rate, the solution on the cathode side will remain saturated with air. It is possible to attain an even higher oxygen concentration in the solution by bubbling pure oxygen rather than air into the chamber, however air was chosen as it is far more convenient to use ambient air outside a laboratory situation.

As described earlier, the bacteria on the anode side have an incredible ability to use carbon as their electron acceptor, however, if there is oxygen available the bacteria will prefer to use the oxygen as an electron acceptor, since it has a lower electrochemical potential. For this reason, nitrogen has been bubbled into the anode chamber to purge the solution for possible oxygen cross over from the cathode chamber, creating an anaerobic environment. Although outside a laboratory situation it is not convenient to purge the anode chamber with pure nitrogen, since nitrogen is not found in nature and would require energy for purification. However in order to achieve more accurate experimental results and enable a better understanding of the MFC system, nitrogen was used in the experiments to purge the anode chamber.



**Table 3.1 - Specific Data from MFC Experiments**

<b>Chambers:</b>	<b>Anode and cathode</b>
Length	3.3 cm = 33 mm
Diameter	3.9 cm = 39 mm
Projected surface area	11.94 cm <sup>2</sup>
<b>Membrane:</b>	<b>Nafion 117</b>
Thickness	177.8 μm = 0.1778 mm
Projected surface area	11.94 cm <sup>2</sup>
<b>Electrodes:</b>	<b>Anode and cathode</b>
Thickness	0.6 cm = 6 mm
Projected surface area (large)	11.94 cm <sup>2</sup>
Surface/ Volume ratio	10 666*

\* For calculation, see appendix XX

### 3.2 Experiment Case 1

Performed by: Alper Erten, Loni Iverson, et al  
Supervised by: Professor Paul Ronney, University of Southern California  
Location: Department of Aerospace and Mechanical Engineering  
Status: Unpublished

The main objective was to attain knowledge regarding the physical mechanisms controlling the fuel cell. Considerable emphasis was placed on testing the effect of alterations to the fuel cell geometry, and testing how various operating conditions affected the overall functionality of the fuel cell. The experiment numbers mentioned in the text does not correspond to the chronological order of the tests, but are used to describe the results.

#### 3.2.1 Experiment #1

By making a polarization curve for the fuel cell, it was possible to characterize the MFC. A polarization curve is created by measuring the voltage and current through a circuit while gradually increasing the resistance, starting with close to zero and ending with approximately an open circuit.

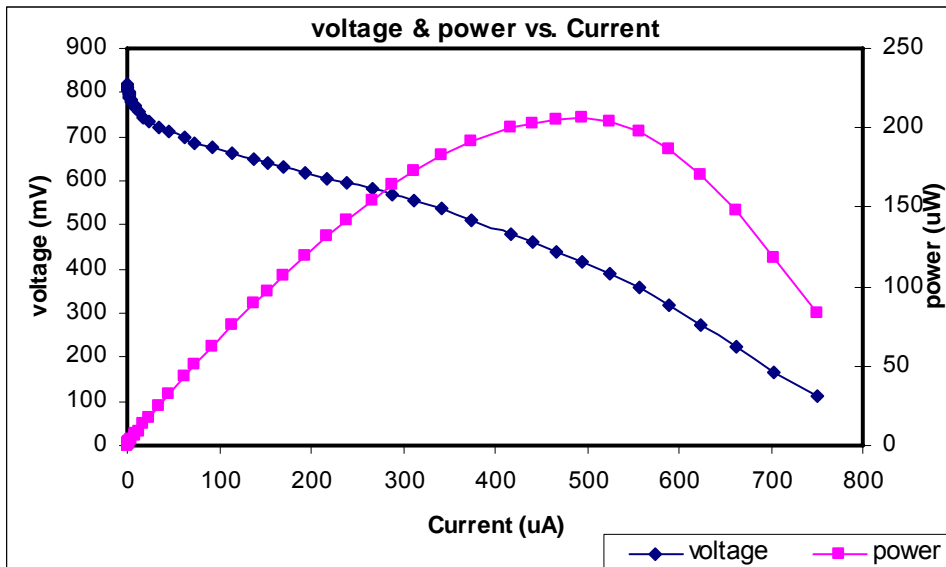
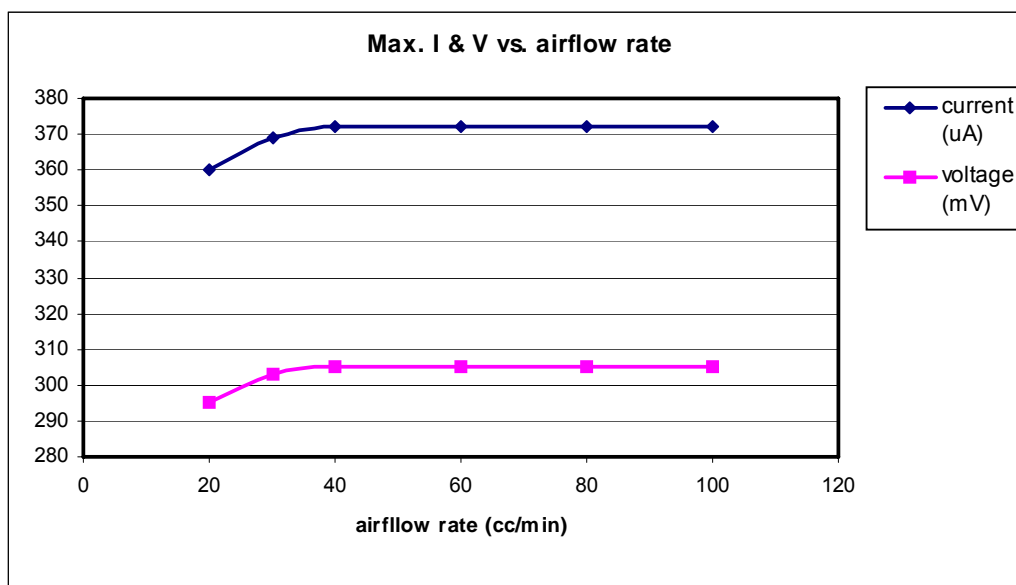


Figure 3.2 - Graphical Presentation of Voltage & Power vs. Current for an MFC

With a projected electrode surface area of  $11.94 \text{ cm}^2$  the max Power attained was approximately 206.4 microwatts. Open Circuit Voltage (OCV) was around 820 mV, whilst the Short Circuit Current (SCC) was measured to be 750  $\mu\text{A}$ .

### 3.2.2 Experiment #2

This experiment is testing airflow at various rates on the fuel cell performance. Max current and voltage is measured while gradually increasing the airflow rate.



The result show that current and voltage increases with increasing airflow rate until it reaches a value of 40 cc/min from where on the power generation stays constant. The experiment is performed with smaller electrodes so the max current is lower than in Experiment #1. However, it is believed the trend is still valid.

### 3.2.3 Experiment #3

Two fuel cells were tested, identical to each other except that the MFC #2 had two platinum wires attached to its anode. On the second day of the experiment various tests were performed, and it showed the following results (Figure 3.3).

- 1) Lactate is injected to the fuel cells and waited for 90 minutes for them to reach maximum power generation.
- 2) N<sub>2</sub> flow to the fuel cells is stopped at 90 mins.
- 3) After waiting for 140 mins the stirrer on mfc#2 is turned on, and in 3 minutes it is seen that the stirring increased the power generation
- 4) After keeping MFC#1 with no nitrogen flow and no stirring for 3 hrs the nitrogen flow is turned back on and an increase in power generation is observed, however this increase was not as much compared to the increase observed with stirring. This shows:
  - a) The stirring bar provides a better a stirring (stronger convection) inside the fuel cell, which is an expected result
  - b) Nitrogen flow has two outcomes, 1: stirring the mixture inside the fuel cell, 2: preventing the oxygen accumulation on the anode side due to cross-over. In this experiment we see that the first outcome of nitrogen flow is an important one, however we cannot see the effect of the second outcome on its own so it's hard to tell how significant the second outcome is.

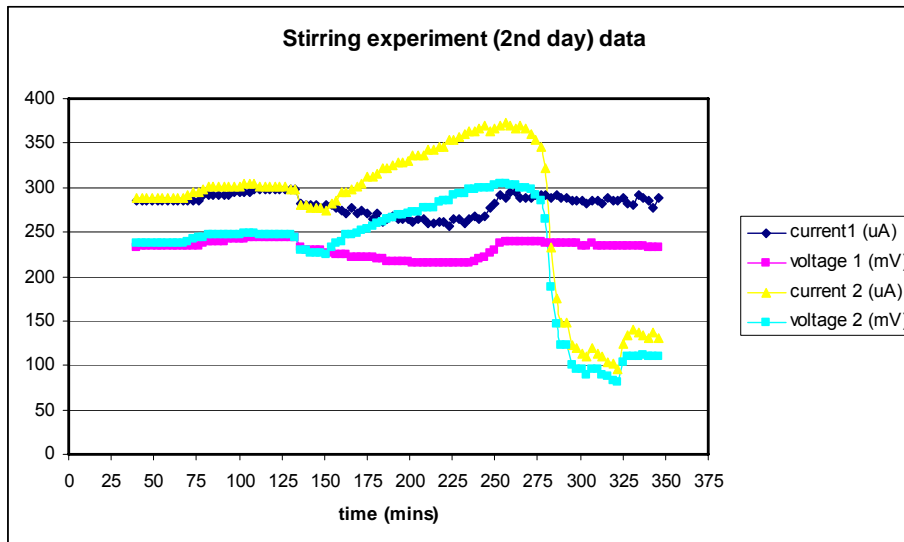


**Figure 3.3 - Stirring Experiment**

In this graph, values for two fuel cells are very close which means using a double wired anode didn't make much difference, still the values for double wired anode was slightly higher.

We see that when the nitrogen flow was stopped it didn't make a big difference and the values for the two fuel cells differ significantly when the second fuel cell is stirred at time 150 mins. At time 275 mins the current and voltage for 2<sup>nd</sup> fuel cell drops quickly while the values for the first fuel remains more stable. We can say that stirring caused the 2<sup>nd</sup> fuel cell consume the lactate quicker than the first fuel cell without stirring. Next at time 325 mins, nitrogen was turned back on mfc#2, so it was both being stirred and flowed nitrogen, turning on the nitrogen increased the power generation by a small amount.

### **3.3 Experiment Case 2**

Performed by: Orianna Bretschger, et al  
Supervised by: Professor Kenneth Nealon, University of Southern California  
Location: Department of Material Science  
Status: Unpublished

The main objective was to gain a better understanding of how the Lactate nutrient decomposes when being used in the MFC under various operating configurations. The purpose was therefore not to maximize the power output, but to measure how the concentration of various species in the fuel cell changes over time.

The fuel cells were injected with a given amount of nutrient at the start of the experiment, but after that there was no additional injections. Small samples of the solution in the anode chamber were extracted at given time intervals throughout the experiment, and the concentration of various species were measured in these samples.

The experiment uses the MR-1 bacteria on the anode electrode, but has no catalyst on the cathode side. Oxygen is used as the electron acceptor at the cathode side, while the anode side is kept anaerobic.

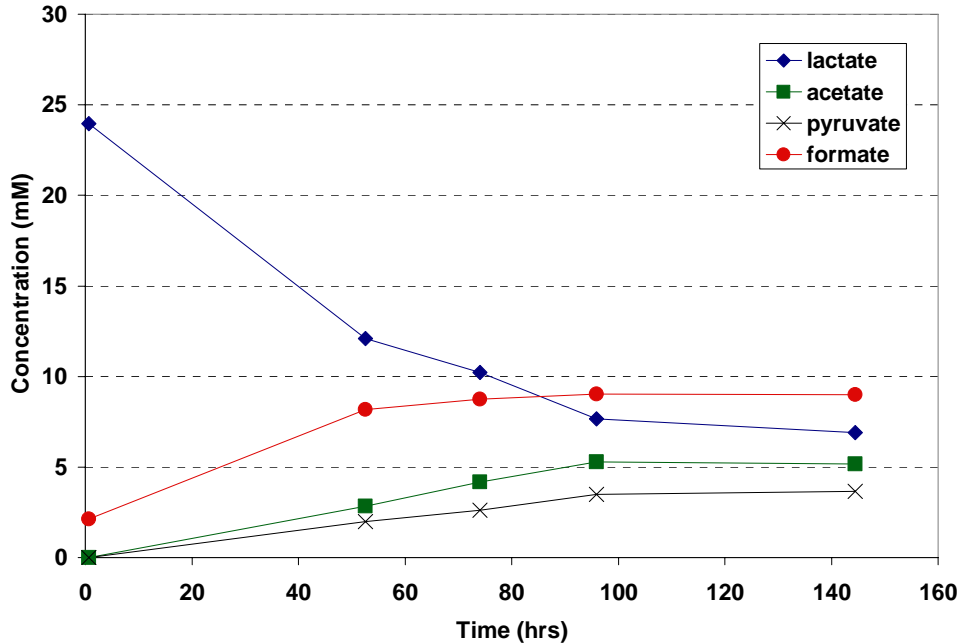


Figure 3.4 - Graphical Presentation of Various Species Concentration in MFC

Although most of the other experiments in this research use platinum on the cathode electrode as a catalyst, it is believed that the data gathered through this experiment will give a fair representation of the decomposition of the nutrient.

The data shows that most of the lactate that is consumed does not become pyruvate, but is converted straight to acetate, formate or other species.

A carbon balance reveals that around 30% of the initial known carbon is not accounted for at the end. Part of this has probably gone to CO<sub>2</sub>, the rest might be various other hydrocarbons.

Table 3.2 - Carbon Balance for nutrient decomposition data

Species	Composition	#C	Start		End	
			mM	mol C/l	mM	mol C/l
lactate	C <sub>3</sub> H <sub>6</sub> O <sub>3</sub>	3	23,96	71,88	6,90	20,71
pyruvate	C <sub>3</sub> H <sub>4</sub> O <sub>3</sub>	3		-	3,66	10,99
acetate	C <sub>2</sub> H <sub>3</sub> O <sub>2</sub>	2		-	5,16	10,33
formate	HCO <sub>2</sub>	1	2,12	2,12	9,00	9,00
<b>Sum</b>				74,00		51,03
Carbons not accounted for at the end						22,97
As a percentage of initial known carbon						32 %

## 4 Governing Equations for MFC FLUENT model

FLUENT is a Computational Fluid Dynamic software, and has been a long time market leader for CFD simulation of fluid flow, heat and mass transfer, and related phenomena including turbulence, reactions, and multiphase flow. The software allows the user to import a geometric mesh of the model being simulated, place boundary conditions on selected cells in the mesh, and then perform calculations on the fluid flow in the full geometry one cell at a time. Even though there is no specific flow in the MFC, FLUID has been selected for its ability to analyze mass transfer, reactions, and include User Defined Functions. In this section, the governing equations within FLUENT will be presented.

### 4.1 Species Calculations in FLUENT

An important variable in the model is the concentration of the various species. The concentrations being used are found both in experimental data from the lab and from literature on similar topics. This section will cover how mass fraction, mole fraction and molar concentration are defined in FLUENT.

Mass fraction is chosen to be the input value for species concentrations in this FLUENT model, and in general mass fractions of all species in a mixture add up to 1. In order to minimize the calculation error in the solver, FLUENT considers the last species in the *Selected species list* under materials as a bulk species. Instead of allowing the user to set a value for the bulk species, the mass fraction of the bulk species is automatically set to 1 minus the sum of the other mass fractions (see equation XX).

$$Y_N = Y_{bulk} = 1 - \sum_{i=1}^{(N-1)} Y_i \quad 4-I$$

$Y_i$  stands for the mass fraction of species  $i$ ,  $N$  is the total number of species and also refers to the last species added to the *Selected species list*. Mole fractions and molar concentrations are calculated by FLUENT using the mass fraction together with specific properties of species. The mole fraction of a species ( $X_i$ ) is related to the



mass fraction from the molecular weight of the species itself ( $M_{w,i}$ ), and the molecular weight of the mixture ( $M_{w,m}$ ), and can be found from:

$$X_i = Y_i \frac{M_{w,m}}{M_{w,i}} \quad 4-II^{10}$$

In general, the molecular weight of the mixture used in the equation can be found by summing up the product of the mass fractions and individual molecular weights for all species in the mixture, and it is denoted kg/kmol (see equation 4-III).

$$M_{w,m} = \sum_{i=1}^N X_i M_{w,i} \quad 4-III$$

However, in highly diluted solutions where the bulk species has a mass fraction of approximately unity, one can assume that  $M_{w,m}$  has the same molecular weight as the bulk species.

The molar concentration of species  $i$  is denoted as  $C_i$  and given in kmol/ m<sup>3</sup>. It can be found by using the mass fraction ( $Y_i$ ) and molecular weight ( $M_{w,i}$ ) of the species  $i$  together with the total density ( $\rho$ ) of the mixture.

$$C_i = \frac{Y_i}{M_{w,i}} \rho \quad 4-IV$$

When using this equation, it is important to remember that the default density calculation method in FLUENT uses the Ideal gas law. However, since the MFC model consists of liquids and gasses dissolved in liquids, it requires a density method designed for non-ideal gasses. The best method is the *Volume-weighted-mixing-law*, which can be selected in the drop down menu for Density under the mixture in the Materials panel. When using this method, FLUENT calculates the density of the

mixture from the mass fractions ( $Y_i$ ) and the respective densities of the species ( $\rho_i$ ), which must be inputted in the material properties.

$$\rho = \frac{1}{\sum_i \frac{Y_i}{\rho_i}} \quad 4-V^{11}$$

Although FLUENT uses the mass fractions to calculate the correct density of the solution, it is sufficient for the user to assume that the density of the solution in MFC is the same as the density of the bulk species in diluted mixtures.

## **4.2 Species and Charge Transportation**

Species and charge transportation are two different, but closely connected, types of transportation that are necessary in the MFC model. Species refers to nutrient, oxidizer, and various other products. The charge transportation refers mainly to the transportation of  $H^+$  ions through the membrane and electrons transported in the electrical circuit.

There are three different transportation processes that normally are preset in a fuel cell, and they are always a response to some sort of force<sup>12</sup>. These processes are diffusion, convection and conduction (see Table 4.1). Diffusion is driven by the concentration gradient of species ( $\frac{dC_i}{dx}$ ), and is connected to the Diffusivity coefficient ( $D$ ) of the species. Convection is a result of pressure differences ( $\frac{dp}{dx}$ ), often caused by a pump, and the transportation is connected to the viscosity ( $\mu$ ) of the species. Conduction is driven by an electrical potential gradient ( $\frac{dV}{dx}$ ), and is connected to the conductivity ( $\sigma$ ) of a material.

**Table 4.1 - Transportation Processes Relevant to Fuel Cells<sup>13</sup>**

Transport Process	Driving Force	Coupling Coefficient	Equation
Diffusion	Concentration gradient, $\frac{dC_i}{dx}$	Diffusivity, $D$	$J = -D \frac{dC_i}{dx}$
Convection	Pressure gradient, $\frac{dp}{dx}$	Viscosity, $\mu$	$J = \frac{Gc}{\mu} \frac{dp}{dx}$
Conduction	Electrical potential gradient, $\frac{dV}{dx}$	Conductivity, $\sigma$	$J = \frac{\sigma}{ z_i F} \frac{dV}{dx}$

However, the MFC has atmospheric pressure in both chambers, which means there are no longitudinal pressure differences. In addition, the scale of the fuel cell is so small that the height difference in the fuel cell will not create any changes in pressure due to gravitational forces. And, since there are no pumps connected to the MFC in order to produce a fluid flow, the mechanical driving forces can be ignored.

Additionally, conductivity is only related to the charged species and not for species in general.

#### 4.2.1 Species Transportation in FLUENT

FLUENT uses a convection-diffusion conservation equation to calculate and predict the local mass fraction ( $Y_i$ ) for each species in each cell in the model. The general conservation equation is given as<sup>14</sup>

$$\frac{\partial}{\partial t}(\rho Y_i) + \nabla \cdot (\rho \vec{v} Y_i) = -\nabla \cdot \vec{J}_i + R_i + S_i \quad 4\text{-VI}$$

Where  $R_i$  refers to the net rate of species  $i$  that is produced by chemical reactions, and  $S_i$  refers to the rate of creation due to various sources in the model.  $\vec{J}_i$  stands for the diffusive flux due to concentration gradients. Since the system is assumed to be in steady state, the transient part of the equation can be neglected:

$$\frac{\partial}{\partial t}(\rho Y_i) = 0 \quad 4\text{-VII}$$

And given that there is no convection or bulk motion of fluids in the MFC,  $\bar{v} = 0$ , gives:

$$\nabla \cdot (\rho \bar{v} Y_i) = 0 \quad 4\text{-VIII}$$

The simplified conservation equation then becomes

$$\nabla \cdot \bar{J}_i = R_i + S_i \quad 4\text{-IX}$$

The diffusive flux is calculated in various ways, depending on how the diffusion coefficients ( $D_{i,m}$ ) are defined. By default, FLUENT uses *dilute approximation*, which allows each species to be given a specific diffusion coefficient. The mass diffusion flux for laminar flows is then defined as

$$\bar{J}_i = -\rho D_{i,m} \nabla Y_i \quad 4\text{-X}$$

FLUENT also allows for a simpler diffusion model called *constant dilute approximation*, which only allows one single diffusion coefficient for the mixture as a whole ( $D_m$ ). Or alternatively if more accuracy is required, it is possible to use *full multicomponent diffusion* which takes into account all the individual binary diffusion coefficients between every pair of species. However, this is very computationally expensive and unnecessary for dilute mixtures, since it will not affect the results significantly. It is also possible to implement specific diffusion calculations for turbulent flows in FLUENT, however in the initial MFC model turbulent diffusion will be calculated manually and implemented by updating the general diffusion coefficient.

### **4.2.2 Charge Transfer**

There are two types of charges that need to be transported in the MFC system, H<sup>+</sup> ions and electrons. Both the ions and electrons are produced at the anode electrode, and need to be transported over to the cathode electrode. As previously mentioned, there are two transportation processes that promote charge transportation in the MFC, which are conduction and diffusion. In the initial MFC model, most of the electrical properties of the fuel cell will be estimated by external calculations, and the electrons will therefore not be taken into account as a species but rather assumed to have the same production and consumption rates as the H<sup>+</sup> ions.

Further more, the initial model will not include the electrical driving forces acting between H<sup>+</sup> ions as a method of transportation, making the assumption that the transportation is achieved solely by diffusion. Because of this, the transportation of H<sup>+</sup> ions is calculated in the same way as non-charged species. However, since it has a very low molecular weight it has a much higher diffusion coefficient, and therefore better transportation properties.

Later versions of the model may include User Defined Functions (see section 6.4) that impose a special transfer of charged species depending on their charge and concentration, or possibly an additional increase in the diffusivity in order to account for the conductive transportation processes. Once the regular electrical system has been implemented it is also possible to model the effect of the electrical conducting nano wires<sup>6</sup>.

### **4.3 Reaction Equations**

FLUENT is equipped to make use of various reaction and combustion models, and even though the bacteria reaction occurring at the anode electrode is a biological reaction, it is believed that the reaction can be approximated to fit the laminar finite-rate model which is normally used on pure chemical systems, for example laminar flames. In all fuel cells there are two main reactions, where one is an oxidation reaction producing electrons at the anode side, and the other is a reduction reaction on

the cathode side consuming electrons. Since both reactions include transmissions of electrons, which cannot be transported through the solution, the reaction can only occur in contact with the electrode. This can be done either with a zone restricted *volumetric reaction* in the electrodes, or possibly more accurately with a *surface reaction* on the electrode surface.

### 4.3.1 Volumetric Reactions

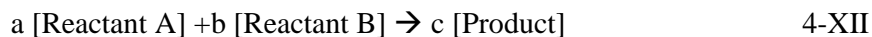
The best known reaction kinetics within combustion theory is based on the Arrhenius expression<sup>15</sup>, which states that the forward rate constant of a reaction is given by

$$k = k_0 e^{-E/\hat{R}T} \quad 4\text{-XI}$$

Where  $k_0$  is the pre-exponential factor and  $E$  is the activation energy for the reaction. From this it can be seen that the reaction rate is a strong function with respect to temperature.

However, in the initial MFC model the reaction rates will be assumed to be unaffected by temperature in the temperature regime that is being used. To further simplify the modeling it is also assumed that there is no activation energy. This means that the forward rate constant is equal to the pre-exponential factor.

When finding the actual reaction rate, the forward rate constant must be seen in relation to the concentration of the reactants in the reaction. Given the general reaction



and a forward rate constant of  $k$ , the net production rate of species C can be found from<sup>16</sup>

$$\Gamma_{\text{Product}} = c k [\text{Reactant A}]^a [\text{Reactant B}]^b \quad 4\text{-XIII}$$

Note that if the reaction is reversible, a competing backward rate constant and reaction would also need to be calculated. At a certain temperature and concentration level the two reactions would cancel each other out, leading to a thermodynamic equilibrium. However, the MFC reactions in this research are assumed to be non-reversible reactions.

Both of these equations are implemented into the FLUENT system in very general terms. The Arrhenius expression for the  $k_{f,r}$  forward reaction rate coefficient is in FLUENT given by

$$k_{f,r} = A_r T^{\beta r} e^{-E_r/RT} \quad 4\text{-XIV}^{17}$$

Where  $A_r$  is the pre-exponential factor (with consistent unit),  $\beta r$  is the temperature exponent (dimensionless),  $E_r$  is the activation energy for the reaction (J/kmol) and  $R$  is the universal gas constant (J/kmol-K). And since MFC reaction rates are assumed unaffected by temperature ( $\beta r=0$ ) and without activation energy, the forward rate constant simplifies to:

$$k_{f,r} = A_r \quad 4\text{-XV}$$

The net reaction rate for species  $i$  for a non-reversible reaction  $r$  is given by the finite rate model in FLUENT to be

$$\hat{R}_{i,r} = \Gamma (v''_{i,r} - v'_{i,r}) \left( k_{f,r} \prod_{j=1}^N [C_{j,r}]^{n'_{j,r} + n''_{j,r}} \right) \quad 4\text{-XVI}^{18}$$

$N$  = number of chemical species in the system

$v'_{i,r}$  = stoichiometric coefficient for reactant  $i$  in reaction  $r$

$v''_{i,r}$  = stoichiometric coefficient for product  $i$  in reaction  $r$

$C_{j,r}$  = molar concentration of species  $j$  in reaction  $r$  (kmol/m<sup>3</sup>)

$n'_{j,r}$  = rate exponent for reactant species  $j$  in reaction  $r$

$n''_{j,r}$  = rate exponent for product species  $j$  in reaction  $r$

$\Gamma$  = represents the net effect of third bodies on the reaction rate

$(v''_{i,r} - v'_{i,r})$  gives the number of how many moles of species  $i$  that is produced or consumed per reaction that occurs. In elementary reactions  $n'_{j,r}$  and  $n''_{j,r}$  are normally equal to the value in front of the species in the reaction. But, for global reactions they may be different in order to reflect the complete reaction.

The net source of species  $i$  due to reactions can be found by looking at all of the  $N_R$  different Arrhenius reactions that include this species:

$$R_i = M_{w,i} \sum_{r=1}^{N_R} \hat{R}_{i,r} \quad 4\text{-XVII}$$

Where  $M_{w,i}$  is the molecular weight of the species  $i$ .  $\hat{R}_{i,r}$  is given in  $\text{kmol/m}^3\text{-s}$ , and  $R_i$  is given in  $\text{kg/m}^3\text{-s}$ . Since the concentration of the species, and therefore also the reaction rates, varies throughout the MFC, it is required to take the integral over the whole reacting area in order to find the total reaction rate (production or consumption) of species in the MFC.

$$R_{i,tot} = \int_0^x R_i(x) dx \quad 4\text{-XVIII}$$

As will be discussed later, it is advantageous to calculate the rates on a per projected area unit, since it makes it easier to compare with other MFC's.

### 4.3.2 Surface Reactions

In a CFC both the anodic and cathodic reaction are surface reactions, and using platinum as a catalyst in order to lower the activation energy required for the reaction. It is believed that the MFC reactions will work in a similar manner, where the bacteria will work as a catalyst on the anode side and drastically increase the rate of the biomass decomposition. In addition, since this MFC is a mediator-less fuel cell, the electrons that are being passed over from the anode chamber to the cathode chamber



do not have the ability to move freely in the solution. In order for these reactions to take place there has to be some contact with the electrodes. Therefore, it is assumed that the reactions occurring on the anode side are better represented as a surface reaction, where the bacteria are believed to be connected to the surface of the porous anode electrode.

Even though FLUENT does allow for the implementation of surface reactions, the initial MFC model has mostly used volumetric reactions because of the simpler modeling theory. However, a quick but rough conversion between volumetric reactions and surface reactions can be used to get a better understanding of the surface reactions required.

In volumetric reactions the forward rate coefficient is given on a per volume basis, whilst the surface reaction naturally is given on a per area basis. Since the electrodes in a fuel cell are permeable, they can be model by using FLUENTs *porous media* function. Porous media has several variables that can be selected by the user, where two of the most important ones for this research are the porosity and the surface/volume-ratio. The porosity is a value ranging from 0 to 1 and represents the volume fraction of fluid, or open area, inside the porous region. The surface/volume ratio is a value representing the active surface area in an electrode on a volume basis. In practice, these two values are closely connected, and interconnected also by the structure of the porous media. However, in FLUENT these two variables are treated as separate input variables, and the structure of the porous media is not taken into account. The two values are normally supplied by the electrode manufacturer, but can also be ascertained by measurements.

The simplest conversion between surface reaction ( $\hat{r}_s$ ) and volumetric reaction ( $\hat{r}_v$ ) can therefore be found by using only the surface/volume-ratio ( $R_{sv}$ ).

$$\hat{r}_v = \hat{r}_s * R_{sv} \quad 4\text{-XIX}$$

However, it is needless to say that the proper conversion will need to take into more factors, such as species deposition on the surface, flow patterns in the porous media, and possibly reaction site species on the surface symbolizing the bacteria.

## ***Electrical Model***

For this first MFC model, the electrical modeling was done through external calculations. The specific diffusion-reaction model of the MFC was first simulated in FLUENT, and then the results were analyzed and converted into more useful energy units.

In general the MFC, like most other energy generators, have two boundary conditions. The first boundary arises if the resistance in the electrical circuit becomes infinitely large, which will result in no electrons going through the circuit. Electrons will build up in the anode chamber until the electro potential difference between the anode and cathode chamber is so large that it is not beneficial for the bacteria to continue and supply electrons. The voltage that is obtained is equal to the maximum voltage of the fuel cell, and is referred to as the Open Circuit Voltage (OCV). The second extreme is achieved if the resistance is decreased to zero, which will encourage all available electrons to pass through the electrical circuit. However, since the reaction rate at the anode electrode is limited by both the transportation of nutrient and the bacteria activity, the availability of electrons will be limited. The current that is set up when the resistance is set to zero is referred to as the Short Circuit Current (SCC), and is the maximum current that the MFC can generate.

Since max current gives a voltage of zero, and max voltage gives a current of zero, these states does not give a complete understanding of the fuel cell functionality. The best value to describe a fuel cells functionality would therefore be the power, which is defined as voltage  $\times$  current and gives the maximum utilization of the fuel cell. However, in order to simplify the first MFC model, the model only aims at simulating the short circuit current.

In general, the bacteria in the MFC decompose nutrient into some sort of “waste product” and produces  $H^+$  ions and electrons. The  $H^+$  ions pass through the PEM (membrane) to the cathode electrode, whilst the electrons are forced to go through an electrical circuit in order to reach the same cathode electrode. The energy that can be utilized as electricity comes from the electrons going through this circuit.

In stead of modeling the electrons directly, the model assumes that every  $H^+$  ion that is produced at the anode also release an electron. And because of the short circuit assumption, there is no resistance for electrons to pass through the electrical system, which means that all electrons are readily available at the cathode electrode for a reduction reaction as soon as the  $H^+$  ions manage to come through the PEM (membrane). Therefore, the model assumes that every  $H^+$  ion that is consumed at the cathode electrode also must have yielded an electron that has already been through the electrical system. This way, the electrical current can be found as a linear relationship of the cathodic reaction rate.

At steady state the production rate of  $H^+$  ions at the anode, must be the same as the consumption rate of the  $H^+$  ions at the cathode. The production and consumption rates are found from the rate of the oxidation and reduction reactions, together with the # of  $H^+$  ions that are produced or consumed per reaction that occurs. If the anodic oxidation reaction emits 4  $H^+$  ions per molecule nutrient, the  $Z_a$  will be equal to 4. Similarly,  $Z_c$  is set equal to the number of  $H^+$  ions that are consumed per cathodic reduction reaction. In order for the system to balance out, the relation between the reactions needs to be:

$$\hat{r}_a = \frac{Z_a}{Z_c} \hat{r}_c \quad 4\text{-XX}$$

Now, assuming that the reactions agree with the relation and a steady state is attained, the amount of electrons going through the electrical circuit is the same as the charge flux of  $H^+$  ions going through the membrane. This flux must at steady state be the same as the amount being consumed at the cathode. This can be found by equation XX.

$$J = Z_a \cdot \hat{r}_a \cdot V_a = Z_c \cdot \hat{r}_c \cdot V_c \quad 4\text{-XXI}$$

The reaction rates  $\hat{r}_a$  and  $\hat{r}_c$  [kmol/m<sup>3</sup>s] refers to the average anodic and cathodic reaction rates in the electrodes, and  $V_a$  and  $V_c$  [m<sup>3</sup>] refers to the total volume of each electrode. In order to convert this into electrical current it needs to be multiplied by

Faraday's constant  $F$  ( $9.6485 \cdot 10^7$  C/kmol), which gives the current ( $I$ ) in a unit of Coulomb/sec, better known as Ampere.

$$I = Z_c \cdot \widehat{r}_c \cdot V \cdot F \quad 4\text{-XXII}$$

Fuel cells have a linear relationship between total power production and the membrane surface area. Therefore, in order to make comparisons between different sized fuel cells it is common to give the power production as a function of membrane area.

Since the preferred unit for fuel cells is made on per membrane area base, the current will be divided by the surface area of the membrane, which in practice changes the volume of the electrode into the thickness of the electrode ( $x$ ). The unit of the current flux ( $i$ ) is  $[A/m^2]$ , whilst it for most MFC will be preferable to scale the unit into  $[uA/cm^2]$

$$i = \frac{Z_c \cdot \widehat{r}_c \cdot V \cdot F}{A} = Z_c \cdot \widehat{r}_c \cdot F \cdot x \quad 4\text{-XXIII}$$

This equation assumes a Columbic efficiency of 100%, which means that every electron that is emitted from the nutrient actually yields electrical power. The value for the average reaction rate is found by exporting the FLUENT reaction rates into an ASCII file, and using Excel to analyze the data and taking an average of the specific reaction rates present in the electrodes.

#### **4.4 Membrane**

When modeling the membrane, there were two various methods that seemed promising. The first method utilized FLUENT's internal Porous Media function, where the user can implement various details about the porous media and thereby achieve a simple but functional membrane between the anode and cathode chamber.

The second method utilizes information on how the Proton Exchange Membrane works, and models the basic function of the membrane. In general, the membrane is a semi-permeable divider between the anode and cathode chambers that has a special ability to allow H<sup>+</sup> ions to pass through, while strongly limiting the flow of other species. This behavior resembles the effect diffusivities have on species. A high diffusivity allows the species to move fast, and the species concentration will level out fast. For a species with a low diffusivity it will take a long time to move from one side of a chamber to the other.

When using diffusivity to define the membrane, the flux of species through the membrane zone can be calculated by using the equation from Table 4.1:

$$J = -D \frac{dC_i}{dx} \quad 4\text{-XXIV}$$

More specific information can be found in section 5.5.2.

## 5 Selecting Appropriate Models and Values

The appropriate models and input values were found based on the experiments previously described and other literature. This section will describe the methodology of how the models and values were found, followed by a table short summary of all the variables.

### 5.1 Dimensions

The dimensions for the MFC computational model were based directly on the experimental data from Case 1 (section 3.2). Some assumptions and simplifications were however made, in order to make the model easier to work with.

Even though the chambers are slightly asymmetric, the model assumed both chambers to be 19.5mm in radius and 33mm long. The electrodes were 6mm thick, and were assumed to have the same radius as the chamber, 19.5mm. This gave the electrodes a projected surface area of 11.94 cm<sup>2</sup>.

The membrane was squeezed between the two glass chambers, and was therefore given the same diameter as the chambers, resulting in a projected surface area of 11.94 cm<sup>2</sup> and a 19.5mm radius. The membrane thickness is 177.8 um, as stated by the manufacturer.

The surface to volume ratio for the electrodes is normally provided by the manufacturer of the electrodes. However, as this was not the case for the ones being used in the Case 1 experiments, it was necessary to find this value by other means.

The surface to volume ratio is a function of how much free volume there is in the electrode, and how large each pore in the electrode is. The electrodes being used in this experiment are made up of thin graphite wires that are bundled together into a short cylinder (projected surface of 11.94cm<sup>2</sup>, height 0.6cm). The surface to volume ratio for the electrodes was calculated to be 10 666 by using two measurable properties, which were relative density and thickness of the graphite wire. The thickness of the graphite wires was found from microscope pictures, which showed

the thickness to be around 15 $\mu$ m. The relative density of the electrodes is defined as the density of the electrode divided by the density of solid graphite, and was found to be around 0.04 (calculations can be found in Appendix Surface to Volume ratio).

**Table 5.1 - MFC Model Dimensions**

<b>Chambers</b>	
Radius	19.5 mm
Length	33 mm (incl. electrode thickness)
Projected surface area	11.94 cm <sup>2</sup>
<b>Electrodes</b>	
Radius	19.5 mm
Thickness	6 mm
Projected surface area	11.94 cm <sup>2</sup>
Surface/ Volume ratio	10 666
Porosity	0.96
<b>Membrane</b>	
Radius	19.5 mm
Projected surface area	11.94 cm <sup>2</sup>
Thickness	177.8 $\mu$ m ~ 0.178 mm

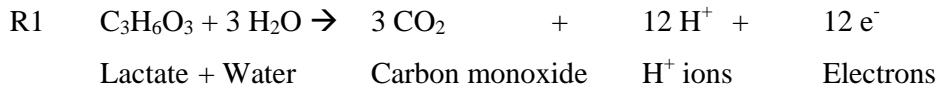
## **5.2 Species and Reaction Mechanisms**

Within combustion kinetics, most conventional chemical reactions are reasonably well understood. By using reaction kinetic databases that have been made with many decades of empirical data, it is possible to achieve fairly accurate numerical solutions. However, the bacterial metabolism of a substance is for many reasons more complex than purely chemical reactions. First of all, the system contains live biological substances that are sensitive and responsive towards changes in the environment surrounding it. Changes in temperature, nutrient and oxidizer availability, or pH level

are all factors that potentially can change the behavior of the bacteria, and possibly alter the concentration of the bacteria. In addition, bacteria are constantly under reproduction, which can result in mutants that react differently to the environment.

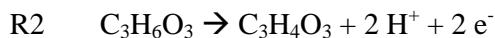
### 5.2.1 Experimental Reactions vs. Modeling Reactions

The overall physical and chemical reaction that takes place in this MFC is lactate being decomposed into H<sup>+</sup> ions, electrons, a resulting waste product and possibly CO<sub>2</sub> and water. The complete decomposition of lactate would be to convert all carbon into CO<sub>2</sub> (see reaction R1)



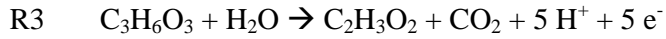
This would require 3 water molecules to be broken down in addition to the lactate itself, and would produce a total of 12 moles of e<sup>-</sup> and H<sup>+</sup> ions per mole of lactate. However, it is not known exactly how, or to what extent, the bacteria decompose the lactate. Plausible products and waste products consist of H<sub>2</sub>O, H<sub>2</sub>, CO, CO<sub>2</sub>, pyruvic acid (C<sub>3</sub>H<sub>4</sub>O<sub>3</sub>), acetate (C<sub>2</sub>H<sub>3</sub>O<sub>2</sub>), formate (HCO<sub>2</sub>), and a multitude of other possible species. While there is constantly being conducted more detailed studies on the *Shewanella* MR-1 metabolism (see 3.3 Experiment Case 2 under Empirical Data), this current computational model will only make use of a very simplified estimation of the metabolism, with a small selection of species.

The # of electrons per anodic reaction, Z<sub>a</sub>, will of course vary depending greatly on what the exact product in the reaction is. If the product is assumed to be pure pyruvic acid (C<sub>3</sub>H<sub>4</sub>O<sub>3</sub>), Z<sub>a</sub> would become 2



If on the other hand lactate is assumed to be converted straight to acetate (C<sub>2</sub>H<sub>3</sub>O<sub>2</sub>), the reaction would consume some water, and would give a Z<sub>a</sub> of 5





The empirical data from Case 2 (section 3.3) shows however that there is no single final product, but that the waste product on the anode side consists of a combination of pyruvic acid, acetate, formate and also a large amount of species that could not be measured.

In order to make an initial computational model, and as a rough approximation of the empirical data, it was assumed that  $Z_a$  would be equal to 4. This means that an average of 4 moles of  $\text{H}^+$  ions and electrons are emitted by every mole of lactate that is consumed at the anode. However, the exact composition of the anode product (the waste) was not taken into consideration.

### 5.2.2 Modeling Species

The initial model uses two reactants, two products, one intermediate product, and one bulk species. The first reactant is the nutrient, or *lactic acid* ( $\text{C}_3\text{H}_6\text{O}_3$ ), whilst the second reactant is the oxidizer, which was assumed to be pure oxygen ( $\text{O}_2$ ).  $\text{H}^+$  ions were used as an intermediate species that was transported through the membrane, whilst the electrons were not initially taken into account in the MFC model, but rather calculated from the reaction rates of other species. As the first product, the remainder of the reactants in the anode was assumed to consist of various products such as pyruvic acid, acetate and formate, but it will be approximated as just one common species, P1. In the cathode chamber water ( $\text{H}_2\text{O}$ ) was produced as product two. Finally, the bulk species in the MFC model, the solution, was considered to consist of pure water ( $\text{H}_2\text{O}$ ). The real MFC would also have nitrogen ( $\text{N}_2$ ) dissolved in the cathode solution in addition to the oxygen, however it can be considered an inert gas in the reactions and was not taken into account in the model.

In order for FLUENT to calculate the molar concentration for the various species in a correct manner, it is important that the molar masses and densities of the species are entered into the material list. The molecular weight was found from the chemical composition together with the molecular weights of the individual atoms. Most of the densities of the species were found Chemfind.com<sup>19</sup>. The density of the lactic acid

was not found in literature, but was estimated to have the same molecular concentration per volume as pyruvic acid, and thereby have a  $90/88 = 1.0227$  times higher density (density pyruvic acid:  $1.2502 \text{ g/cm}^3$ ). The molecular weight of P1 was assumed to be the same as “Lactate – 4 H<sup>+</sup> ions”, whilst the density was approximated to be the same as pyruvic acid.

**Table 5.2 - Properties of Selected Modeling Species**

Species	Name	Composition	MW	Density, (g/cm <sup>3</sup> )
R1	Nutrient, Lactate	C <sub>3</sub> H <sub>6</sub> O <sub>3</sub>	90	(NB approx) 1.278 g/cm <sup>3</sup> = 1.278e3 kg/m <sup>3</sup>
R2	Oxygen	O <sub>2</sub>	32	1.429 (g/L) = 1.429 kg/m <sup>3</sup>
I	Intermediate, H <sup>+</sup> ions	H <sup>+</sup>	1	0.0899 (g/L) = 0.0899 kg/m <sup>3</sup>
P1	“Waste”	“C <sub>3</sub> H <sub>2</sub> O <sub>3</sub> ”	86	1.250 g/cm <sup>3</sup> = 1250 kg/m <sup>3</sup>
P2	Water	H <sub>2</sub> O	18	0.998 g/cm <sup>3</sup> = 998 kg/m <sup>3</sup>
S	Solution, water	H <sub>2</sub> O	18	0.998 g/cm <sup>3</sup> = 998 kg/m <sup>3</sup>

- MW calculated from composition

- Density found from: [www.chemfinder](http://www.chemfinder.com) or <http://en.wikipedia.org/>

Since the model uses a mixture of species diluted in a solution, it is possible to assume that the molecular weight of the mixture is the same as the one for the solution, bulk species (998 kg/m<sup>3</sup>). In order to simplify the creation of the species, all the species are originally based on the properties of H<sub>2</sub>O, just with difference in MW, diffusivity, and density.

## 5.2.3 Reactions and Mechanisms

### Simplified 2-step reaction

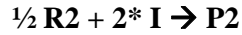
For the initial model the reaction mechanisms were simplified to an absolute minimum, and only comprise the overall reaction without specific details of how the bacteria decompose the nutrient. Since the oxidation and reduction reactions are physically separated by the Nafion membrane, the simplest reaction possible will consist of one reduction reaction and one oxidation reaction. This will be referred to as a simplified 2-step reaction.

- (1) Anodic oxidation reaction



$$\text{Mass balance: } 90 = 86 + 4 \times 1 \quad \text{OK!}$$

(2) Cathodic reduction reaction



$$\text{Mass balance: } \frac{1}{2} \times 32 + 2 \times 1 = 18 \quad \text{OK!}$$

Ideally, both reactions would be surface reactions since they only can occur while being in physical contact with the electrodes. This is due to the electrons that are produced on the anode side needing to be transported through the anode electrode to the cathode electrode where they are consumed. However, the reactions can also be implemented as volumetric reactions that are restricted in a specific volume. This latter method has been used for this master thesis research.

### **Simplified 3-step reaction**

For the MFC to operate optimally, the anode needs to be kept anaerobic. However, it is well known that oxygen to a certain extent can permeate from the cathode side and through the Nafion membrane into the anode chamber. If this occurs, the oxygen will be the preferred electron acceptor for the bacteria, and a third counteracting reaction takes place. In order to take into account the effect of the oxygen cross over, it is possible to use a simplified 3-step reaction that also includes the counteracting reduction reaction.

(3) Counteracting anodic reduction reaction



$$\text{Mass balance: } 90 + \frac{1}{2} \times 32 = 88 + 18$$

The counteracting reaction does not require being in contact with electrodes, and since the reaction can utilize platonic bacteria that are not attached to the electrodes as well, the reaction can theoretically occur throughout the whole anode chamber as a volumetric reaction. However, since most of the bacteria are assumed to be connected to the electrodes, the reaction was modeled as a volumetric reaction with a restricted area in the anode electrode.

## 5.2.4 Reaction rates

The previously mentioned reaction rates have to be either found or estimated before the computational model can be used to predict current.

Of the three reactions that were mentioned, only the cathodic reaction (2) is based on traditional chemical reaction kinetics. This reaction occurs on the cathode electrode, which in these experiments is covered with platinum. Since the computational model assumes that the anode side is the limiting factor, the cathodic reaction has to be fast. By using a high value for the cathode reaction rate, it will assure that all H<sup>+</sup> ions that pass through the membrane on to the cathode will react and instantly turn into water, as long as there is oxygen present. To be on the safe side, the cathodic reaction rate is set to:

$$k_2 = 1e+10 \quad 5-I$$

The anodic oxidation reaction (1), which is caused by the bacteria, is assumed to be the limiting reaction in the fuel cell. This reaction rate cannot be found in literature, however it is believed that it can be calculated using the computational model. By testing various reaction rates, and comparing the simulated results with experimental data, it is possible to find the appropriate rate.

$$k_1 = ? [1/s] \quad 5-II$$

For the 3-step mechanism, which includes oxygen cross over, the reaction rate for the counteracting anodic reduction reaction (3) will also need to be found. It is known that this is a relatively fast reaction, and that given the choice bacteria will always use oxygen as its electron acceptor. Therefore, as an initial guess, this will be set to

$$k_3 = 1e+5 [1/s] \quad 5-III$$

Which should result in all oxygen molecules that pass through the membrane and into the anode chamber will react as soon as they come in contact with nutrient.

### **5.2.5 Next generation reaction mechanisms**

There are several steps that can be made to increase the accuracy of the reaction mechanisms. A description of possible steps is presented below.

#### ***(a) Changing reactions 1 and 2 into surface reactions***

Since the reaction in the electrode requires contact with the electrode, using surface reaction on both electrodes would result in a more accurate model. The model has been tested using anodic surface reaction and cathodic volumetric reaction with good results. However, in implementing dual surface reactions it has proved difficult to export and analyze the reaction rates.

#### ***(b) Model bacteria as surface species on the anode electrode***

The experimental MFC tests all show that the increase in power decreases drastically as the concentration of nutrient rises over a certain threshold. This effect can possibly be modeled by implementing the bacteria as a reacting surface species with a specific coverage on the anode electrode.

#### ***(c) Include negative reaction for nutrient overflow***

Alternatively, the nutrient threshold described in (b) can be modeled by implementing a negative reaction rate that counteracts the regular anodic oxidation reaction once the nutrient concentration rises above the certain threshold. Since this would require a non arrhenius reaction, it might need to be implemented as a source and sink by a UDF (see section 6.4).

#### ***(d) Implement more detailed reaction mechanisms***

As stated earlier, the reaction mechanism is very simplified. In order to make the model more accurate, it is possible to implement more detailed information on the metabolism of the nutrient. Also, it is important to investigate what happens to the waste, since the bacteria possibly can reuse and further decompose some of these species.

### 5.3 Concentrations

#### Lactate, R1

The lactate concentration can be calculated directly from the experimental lab tests. The experimental lab tests have been done in batches, and not as a continuous flow of nutrient. In order to make the calculations easier only the maximum nutrient, at the time just as nutrient has been injected into the anode, will be used.

Initially before injection, the anode chamber has 30 ml of buffer/solution, which is approximated to consist of pure water. At the start of the experiment 1ml of a nutrient solution is injected. This nutrient solution has a 60mM concentration of lactate, and the rest is buffer (water)<sup>20</sup>. After the injection, the molar concentration of the total cathode solution that is lactate can be found by:

$$lactate\_molar = \frac{0.060[mM.lactate] * 1[ml]}{(30 + 1)[ml]} \approx \underline{2mM} \quad 5-IV$$

$$C_{lactate} = 2[mM] * [1000liter / m^3] = 2moles / m^3 = \underline{0.002kmol / m^3}$$

Again, it is beneficial to manually calculate the expected mass fraction ( $Y_{lactate}$ ) and mole fraction ( $X_{lactate}$ ) by using previous equations. The molecular weight of lactate is 90 kg/ kmol.

$$Y_{lactate} = \frac{C_{lactate}}{\rho} M_{w.lactate} = \frac{0.002[kmol / m^3]}{998 \left[ \frac{kg}{m^3} \right]} * 90 \left[ \frac{kg}{kmol} \right] = \underline{1.80 * e^{-4}} \quad 5-V$$

$$X_{lactate} = Y_{lactate} \frac{M_{w.m}}{M_{w.lactate}} = 1.80 * e^{-4} * \frac{18 \left[ \frac{kg}{kmol} \right]}{90 \left[ \frac{kg}{kmol} \right]} = \underline{3.6e^{-5}} \quad 5-VI$$

As stated above, these values correspond to the maximum concentration just as the nutrient is injected into the anode chamber. The concentration will decline as time goes by, since it is consumed by the bacteria. In addition, the effect of waste remaining from the first injections when nutrient is injected the second time, has not been taken into account.

## Oxygen, R2

The oxygen concentration is not measured experimentally, but can be estimated by looking at the experimental setup and comparing to suitable literature. The oxygen is added to the cathode chamber by bubbling air through the solution. In order to simplify the initial model it is assumed that the bubbling of air into the chamber is efficient enough to saturate the water with air.

Given this assumption, there are several resources that describe the oxygen concentration in the solution. General Chemistry Online gives the following equation for dissolved oxygen (DO) in Distilled water at temperatures (T) between 0°C and 30°C, where P is the barometric pressure (torr) and p is the water pressure (torr).

$$DO(T) = \frac{(P - p) * 0.678}{35 + T} \quad 5\text{-VII}$$

At sea level the barometric pressure is 760 torr, and assuming 25°C the water vapor pressure is 23.76 torr. This gives a saturated DO concentration of 8.32 mg/ L. It is assumed that the solution can be approximated to consist of pure water, which gives us a density of 998 g/ L. Inserting this into equation 5-V gives

$$Y_{O_2} = \frac{8.32 \left[ \frac{mg}{L} \right]}{998 \left[ \frac{g}{L} \right] * \left[ \frac{1g}{1000mg} \right]} = 8.337 * e^{-6} \quad 5\text{-VIII}$$

The only value that FLUENT requires the user to enter is the mass fraction. However, the molar concentration and mole fraction should also be calculated manually in order to check the values that FLUENT gives. The molecular weight of oxygen is 32 kg/kmol.

$$X_{O_2} = Y_{O_2} \frac{M_{w.m}}{M_{w.O_2}} = 8.337 * e^{-6} * \frac{18 \left[ \frac{kg}{kmol} \right]}{32 \left[ \frac{kg}{kmol} \right]} = 4.69 * 10^{-6} \quad 5-IX$$

$$C_{O_2} = \frac{Y_{O_2}}{M_{w.O_2}} \rho = \frac{8.337 * e^{-6}}{32 \left[ \frac{kg}{kmol} \right]} * 998 \left[ \frac{kg}{m^3} \right] = 2.6 * e^{-4} \left[ \frac{kmol}{m^3} \right] \quad 5-X$$

These values correspond to the theoretical maximum concentration of oxygen in the cathode chamber if the bubbling of air manages to saturate the solution. However, since air consists roughly of 21% oxygen and 79% nitrogen on mole basis, it is possible to increase the dissolved oxygen level by bubbling pure oxygen in stead of air into the chamber. This is not a practical solution outside the laboratory, since pure oxygen requires energy to be produced.

**Solution, S:**

The mixture is as earlier mentioned assumed to be species diluted in a solution, where the mass fraction of the solution is close to one. The solution itself is approximated to be pure water, and is entered as the last species in the *Selected species list* under materials, which means it is the bulk species in the mixture. Therefore, it is not possible for the user to enter any value that effects the concentration of the solution. However, it is still interesting to do manual calculations to find what values are expected.



Due to the assumptions stated above, both the mass fraction and the mole fraction is expected to be ~1.

$$Y_{solution} = X_{solution} \approx 1 \quad 5\text{-XI}$$

Using the same equations that have been used for the nutrient and oxygen earlier, the expected molar concentration becomes:

$$C_{solution} = \frac{Y_{solution}}{M_{w.solution}} \rho = \frac{1}{18 \left[ \frac{kg}{kmol} \right]} * 998 \left[ \frac{kg}{m^3} \right] = 55.4 \left[ \frac{kmol}{m^3} \right] \quad 5\text{-XII}$$

### **H<sup>+</sup> ions, I**

For the following reasons the user should not alter the concentration of H<sup>+</sup> ions by setting this at a specific value manually. The H<sup>+</sup> ion concentration is recalculated and altered by the model itself for every iteration that is performed. However, it is possible to do feasibility tests on the model by analyzing the concentration the model produces.

The pH value is a measurement of the concentration of H<sup>+</sup> ions in a solution, and is measured in moles per liter solution<sup>21</sup>. The more H<sup>+</sup> ions that are available in the anode chamber, the higher the diffusion of protons through the membrane it is possible to attain. However, the higher the H<sup>+</sup> concentration we get, the lower pH value and more acidic the solution becomes. And, if the solution becomes too acidic, the bacteria will die. Therefore, the pH value can be seen as a tradeoff between higher efficiency and life sustainability of the bacteria.

The general equation for pH is:

$$\text{pH} = -\log_{10} [\text{H}^+] \quad 5\text{-XIII}$$

A neutral pH of around 7 translates into the H<sup>+</sup> concentration of:

$$C_{\text{H}^+} = 10^{-7} = 1e^{-7} \text{ mol/liter} = 1e^{-7} \text{ kmol/m}^3 \quad 5\text{-XIV}$$

Reversing equation XX allows us to find the H<sup>+</sup> mass fraction for pH = 7:

$$Y_{\text{solution}} = \frac{C_{\text{solution}}}{\rho} M_{\text{w.solution}} = \frac{1e^{-7} \left[ \frac{\text{kmol}}{\text{m}^3} \right]}{998 \left[ \frac{\text{kg}}{\text{m}^3} \right]} * 18 \left[ \frac{\text{kg}}{\text{kmol}} \right] = 1.8e^{-9} \quad 5\text{-XV}$$

The molar concentration of H<sup>+</sup> can be found in the FLUENT model, and should be used to check the pH value for the fuel cell. The first version of the MFC model does not take into account the concentration of H<sup>+</sup> ions that is already present in the solution on both sides before the nutrient is injected.

### **Waste, P1**

The waste which is produced as the bacteria consume the nutrient is assumed to be pyruvic acid. It is far from certain that this really is the case. In real life, the maximum concentration of P1 assuming one injection of nutrient is attained if all the lactate is transformed to pyruvic acid. This would mean that the maximum molar concentration that is possible to attain is:

$$C_{\text{waste}} = C_{\text{lactate}} = 3.9 * e^{-3} \left[ \frac{\text{kmol}}{\text{m}^3} \right] \quad 5\text{-XVI}$$

However, since the model is run in a steady state mode assuming a constant feed of nutrient, and there is no reaction that actually removes the waste from the system, the

concentration of waste would theoretically just continue to build up. In order to prevent this, there have been made modifications on the system to drain the waste. This will be explained better in the next section.

### **Water, P2**

Similarly to the waste, the production of water would also be limited to the same concentration as of the lactate that was initially injected into the anode. The same problem is also seen in this case, where the concentration of water would just continue to build up. It should be mentioned that the produced water is in fact the same as the solution, and even though they have two different species name in the model they will in practice mix together. The problem was solved again by doing slight modifications to the model in order to drain the accumulating P2 species, as will be discussed in the next section.

**Table 5.3 - Maximum Species Concentraions**

<b>Species name</b>	<b>Short</b>	<b>Mass fraction <math>Y_i</math></b>	<b>Mole fraction <math>X_i</math></b>	<b>Molar concentration <math>C_i</math> [kmol/ m<sup>3</sup>]</b>
Nutrient (lactate)	R1	$1.80 e^{-4}$	$3.6 e^{-5}$	$2.0 e^{-3}$
Oxygen	R2	$8.337 e^{-6}$	$4.69 e^{-6}$	$2.6 e^{-4}$
Intermediate (H+)	I			
Product1 (waste)	P1			$3.9 e^{-3}$
Product2 (water)	P2			$3.9 e^{-3}$
Solution (water)	S	$\sim 1$	$\sim 1$	55.4

## 5.4 Diffusivities

### 5.4.1 Laminar Mass Diffusion Coefficients

The initial model is strongly affected by mass diffusion, which made it important to use appropriate values for the diffusivity coefficients. Literature research proved it difficult to find exact values, since the coefficients are a function of both properties of the species itself, and the properties of the mixture or solution it is in.

The simplest method of setting the diffusivity in FLUENT is by using the *constant dilute approximation*, which uses only one diffusivity coefficient for all the species in the mixture. Since the system can be viewed as a set of gasses or species dissolved in water, a literature research stated that reasonable values should be around  $2.88e-9$   $m^2/s$ . Which is around 4 orders of magnitude lower compared to gasses that are diffusing in air having a diffusivity of around  $2.88e-5$   $m^2/s$ . This method gives approximate values for the diffusion, but will not contribute any new findings for the system.

The second generation of diffusion coefficients took into account an approximated relative relationship between the modeling species. Smaller and lighter species were assumed to have a higher diffusion coefficient than heavier species. By selecting *Dilute approximation* FLUENT allows the user to insert one coefficient for each species in the mixture ( $D_{i,m}$ ). The new diffusivities were calculated by using the *constant dilute approximation* value as a base, and multiplying with a roughly estimated relative factors based on size difference of the species.

**Table 5.4 - Diffusivity Coefficients based on Approximated Relative Factors**

Species	Name	Relative Factor	$D_{i,m}$ [ $m^2/s$ ]
Base	-	-	$2.88e-9$
R1	Lactate	1	$2.88e-9$
R2	O <sub>2</sub>	30	$8.64e-8$
I	H <sup>+</sup>	100	$2.88e-7$
P1	"Waste"	1	$2.88e-9$
P2	H <sub>2</sub> O	30	$8.64e-8$

<b>B</b>	H2O	30	8.64e-8
----------	-----	----	---------

The third generation of diffusivities is an extension of the dilute approximation, employing new values found in literature. The U.S. EPA (Environmental Protection Agency) states two ways to calculate diffusivity values in one of its technical support documents<sup>22</sup>.

$$D_{a,i} = \frac{1.9}{(MW_i)^{2/3}} [cm^2 / s] = \frac{1.9 \times 10^{-4}}{(MW_i)^{2/3}} [m^2 / s]$$

$$D_{w,i} = \frac{22 \times 10^{-5}}{(MW_i)^{2/3}} [cm^2 / s] = \frac{22 \times 10^{-9}}{(MW_i)^{2/3}} [m^2 / s]$$

5-XVII

The first equation refers to diffusivity of species of that are in air, whilst the second equation refers to species in water. Both diffusivity equations were originally given in cm<sup>2</sup>/s, which is 10000 times higher than the m<sup>2</sup>/s which will be used in the report, and the molecular weight is given in (kg/kmol). Notice that the equation for water gives a value 4 orders of magnitude lower than the one for air. The U.S. EPA method for diffusivities of species in water gives the values found in Table 5.5 for laminar diffusion coefficients for the selected modeling species, which seem to correspond to the same general pattern as estimated with the two previous methods.

**Table 5.5 - U.S. EPA Laminar Diffusion Coefficients**

<b>Species</b>	<b>Name</b>	<b>MW</b>	<b>D<sub>i,m</sub> [m<sup>2</sup>/s]</b>
<b>R1</b>	Lactate	90	1.10E-09
<b>R2</b>	O2	32	2.18E-09
<b>I</b>	H+	1	2.20E-08
<b>P1</b>	"Waste"	~90	1.10E-09
<b>P2</b>	H2O	18	3.20E-09
<b>B</b>	H2O	18	3.20E-09

### 5.4.2 Turbulent diffusion

The initial test of the model showed that the diffusivity in the anode and cathode chamber was a very limiting factor in the current production. From the basic working assumptions, the limiting factor of the fuel cell should be the anodic reaction rate, and not the diffusivity. In order to check this, a more thorough analysis on the diffusivities was carried out.

As mentioned earlier, the two chambered MFC that is used for the tests does not have a continuous flow of fluid, and should therefore be controlled by diffusion and electrical driven forces. However, a new inspection of the MFC experiment shows that the bubbling of various gases into the anode and cathode chamber possibly causes the liquid to mix more rapidly than it normally would. This effect can be seen as turbulent mixing, or turbulent diffusion.

In order to find out whether the bubbling has significant influence on the mixing, or if its effect is negligible, simple tests and calculations were performed.

To simplify the model, the turbulent diffusion coefficient can be roughly estimated by using the bubbling speed and the dimension of the chamber. The actual chamber thickness can be used as the diffusion layer thickness.

$$D_T = 0.06 * u' * L_I \quad 5\text{-XVIII}$$

$u'$  is the turbulence intensity and can be estimated by as:

$$u' = 0.1 * U \quad 5\text{-XIX}$$

$L_I$  is the integral length scale of turbulence, using  $d$  the shortest dimension of the chamber, either diameter or axial length. The shortest dimension in the chambers tested is the axial length, which is 33mm long, or  $3.3 * 10^{-2}$  m.

$$L_I = 0.5 * d = 0.33 / 2 = 0.0165 \text{ m}$$

5-XX

The gas bubbling is controlled by the flow of the gas injected into the anode and cathode chamber, which again is controlled by the settings on the rotameter connected to each gas tank. Bubbling speed was measured by video filming the anode and cathode chamber while the gas was bubbling into the chamber at different flow rates.

**Table 5.6 - Bubble Speed**

<i>Gas Flow Rate (cc/min)</i>	10	20	30	40
Bubbling Speed (m/s)	0.156	0.195	0.195	0.26

Reference Alper Erten, Case 1

In most of the experiments conducted, the gas flow rate had been approximately 20 cc/min, giving a velocity of around 0.2 m/s (see Table 5.6). The turbulent diffusion coefficient gives:

$$D_T = 0.06 * (0.1 * 0.2 \text{ m/s}) * (.0165 \text{ m}) = 1.98 \times 10^{-5} \text{ m}^2/\text{s} \quad 5-XXI$$

Since the regular diffusion in the MFC was calculated to be around =  $2 \times 10^{-9} \text{ m}^2/\text{s}$ , the turbulent diffusion created by the bubbling gasses was around 10 000 times higher. This has a considerable effect on the transportation conditions in the fuel cell. Therefore a turbulent diffusion coefficient of  $1.98 \times 10^{-5}$  was added together with the laminar diffusion coefficient in both the anode and cathode chamber. It was assumed that the turbulent mixing only occurs in the chamber, and that it does not alter the diffusion in the two electrodes or the membrane.

## 5.5 Membrane

There were two initial ideas of how to model the membrane. The first one was to use FLUENT Porous Media function, and the second was to look at the membrane's actual species transportation properties.

### 5.5.1 Porous Media

Selecting the membrane zone in FLUENT, and using the Porous Media function, seemed the easiest way to implement the MFC membrane. It allows the user to insert values for the porosity of the membrane, and also allows the user to insert various viscous and inertial resistances.

Because of its simplicity, this model initially seemed a good way to model the MFC. However, after using the Porous Media function for a while, it appeared this function was more relevant for models where there actually is a flow existing, rather than our diffusion controlled system. Due to the Porous Media function lacking the possibility to modify and control the detailed mass transportation, it was eventually decided to stop using it.

### 5.5.2 Diffusivity Reducing Media

The second method of modeling the membrane is based on its transportation properties. The function of the membrane is to separate the anode and cathode chamber, and allow only selective species through whilst blocking out the rest. Of course, no membrane is ideal, which means that there still will be resistance for the wanted species to pass through, and species that are not wanted will also managed to pass through, though hopefully in a smaller degree. This first MFC model has a focus on transportation based on concentration gradients, and it was therefore natural to investigate the diffusion properties of the Nafion membrane.

For the initial MFC model the membrane was simplified into becoming a zone with selective diffusivities depending on the species. The lower the diffusivity in the zone is, the more difficult it is for species to penetrate through the membrane. In order to make the basic simulations as easy as possible, it was decided that the membrane should block all species except the intermediate species ( $H^+$  ions). However, since FLUENT does not allow diffusivities of zero, the diffusivity was set at  $1e-22 \text{ m}^2/\text{s}$  (around 12 orders of magnitude lower than the laminar diffusion).

In order to find data on the transportation of  $H^+$  ions through the membrane, a literature research was performed. A recent research paper from University of Miami



gave simulated diffusion coefficients of H<sup>+</sup> through a Nafion 117 membrane that was based on an atomistic simulation. The data was also correlated with experimental data, and had proved to have an accuracy of at least 50% at room temperature.

**Table 5.7 - Simulated Diffusion Coefficients of H<sup>+</sup> ions in a Nafion 117 membrane<sup>23</sup>**

Water content, $\lambda$	Relative humidity	$D_{H^+}$ , cm <sup>2</sup> /s
3 (Low)	50%	$6.0 \times 10^{-7}$
13 (High)	100%	$3.4 \times 10^{-6}$
22 (High)	Liquid water	$5.0 \times 10^{-6}$

Atomistic Simulation of Conduction and Diffusion Processes, Nafion Polymer Electrolyte, Experimental Validation

The water content in Nafion is a function of the relative humidity. The values from Table 5.7 refers to diffusivities at room temperature. Since the MFC model assumes that there is solution in both the anode and cathode chamber which is approximated to consist of pure water, the correct water content is  $\lambda = 22$ . The reason the diffusivity of H<sup>+</sup> ions is so strongly connected with the water content in the Nafion membrane is because most of the ions are transported together with the water.

In the 3-step reaction modeling, where a counteracting anodic reaction with oxygen is being studied, oxygen will be allowed to diffuse through the membrane in addition to the H<sup>+</sup> ions. The cross over diffusivity of oxygen was found from in a research paper which analyzed gas crossover implications. The oxygen crossover diffusivity from this report was also compared to results from various other papers, which showed that there is a large difference between papers. However, most of the values for the oxygen crossover were in the same region as the paper used (ranging from 0.24 and up to 1.9 cm<sup>2</sup>/s).

Diffusivity of oxygen in Nafion 117<sup>24</sup>:

$$D_{O_2} = 0.62 * 10^{-6} \text{ cm}^2/\text{s} = 0.62 * 10^{-10} \text{ m}^2/\text{s} \quad \text{5-XXII}$$

The internal equation that FLUENT uses to calculate the diffusivity is based on the diffusivity equation in Table 4.1:

$$J = -D \frac{dC_i}{dx} \quad \text{5-XXIII}$$

## 5.6 Power Estimations

The MFC computational model is based on the Case 1 (Section **Error! Reference source not found.**) experimental set up. Therefore, the expected power, current and voltage estimations should correspond to the results from these experiments.

From the experimental data acquired from Case 1, section **Error! Reference source not found.**, the Short Circuit Current (SCC) is measured to be 750uA for an electrode with 11.04 cm<sup>2</sup> surface area. This results in an experimental current flux of around 67.9 uA/ cm<sup>2</sup>. Since this is our aim for the computational model, the reaction rates of the anode and cathode side can be estimated in such a way that the model initially gives the right result for the base case.

$$i_{\text{experimental}} = \frac{750\mu\text{A}}{11.04\text{cm}^2} = \underline{67.9\mu\text{A} / \text{cm}^2} \quad 5\text{-XXIV}$$

Once the required reaction rates have been achieved with the model it is possible to analyze the results, and try to find the various limitations and possible design improvements.

## **6 Setting up and Running the MFC model in FLUENT**

### **6.1 Computer Lab**

In order to get the most computational power, the computer lab was set up with three separate computers running individual versions of FLUENT, which were connected to a single shared screen, keyboard and mouse through a “4 computer switch”. In addition, a separate portable computer was equipped with a full set of the software to simplify alterations of the model and analyzing results while the model was running. All the computers were connected together through a local network in order to allow for file and result sharing.

### **6.2 Geometry in GAMBIT**

Before simulations can be performed in FLUENT, a geometric model has to be made. This can be done in a large range of different meshing programs. The program that was selected for this master thesis research was GAMBIT, which is also the program recommended by FLUENT.

Production of the geometric model can be divided into three separate stages; *geometry, meshing and zone selection*.

#### **6.2.1 Geometry and Zones**

When transferring the geometry of a physical model into the GAMBIT program, it is important to remember that the simpler the geometry is constructed, the faster the calculations can be performed. This does not mean that important details in form or shape should be neglected, but if it is possible to simplify the geometry it will save time to do this.

One simplification that is easy to do is locating symmetry lines. If the physical model is symmetric over an axis, and there are no physical differences between the two sides, it would be computational smart to only calculate one half of the model. The MFC model that are being tested can in the simplified model be seen as symmetric

over the center axis, and therefore only the top half of the MFC was modeled. In addition, in stead of modeling a full half cylinder, it is possible to only to a slice in the cylinder, and explain to FLUENT how to calculate the rest of the cylinder by selecting Axisymmetric solver. This will be described in more detail in the *Solver Settings* section.

In general, all geometries in GAMBIT are subject to a hierarchy of various types of inputs. The most basic input which is lowest in the hierarchy is the *Vertex*. A vertex is a single point in space, that has a specific location relative to a fixed coordinate system (i.e. 1,1,0, where 0,0,0 would be the origin). The next level in the hierarchy is an edge, which is a line connecting to vertexes (1,1,0  $\rightarrow$  2,1,0). By joining together a minimum of 3 edges it is possible to make a face, and by connecting minimum 4 faces it is possible to create a volume. Volume is the highest level in hierarchy, and is only possible to use if the model is being drawn in 3D. If the model is going to be used as a 2D model, faces are the highest level.

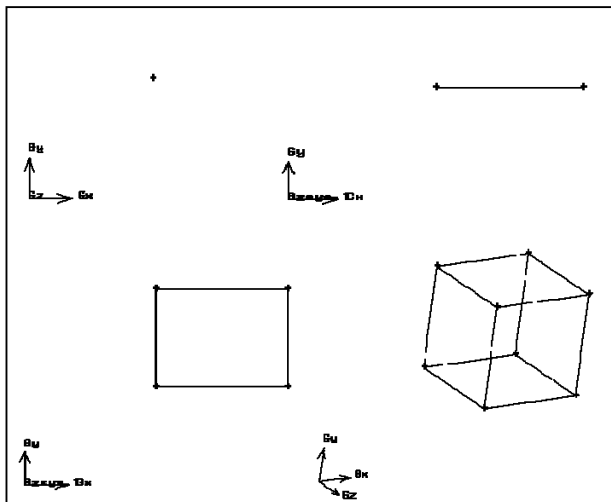


**Figure 6.1 - GAMBIT Layers**

The geometric model that has been used for the initial MFC model has been a 2 dimensional model, which also can be used as a 1 dimensional model for the first tests. Each separate part in the MFC was created as a separate zone in the model, where each zone was represented by a face in the 2D model. Therefore, the finished 2D model included 5 faces as seen in Figure 6.1. The fuel cell was designed as 1

point in the GAMBIT coordinate represented 1 mm in real life, and the complete fuel cell measured  $L=66.178$  mm and  $W=19.5$  mm (though this is the radius).

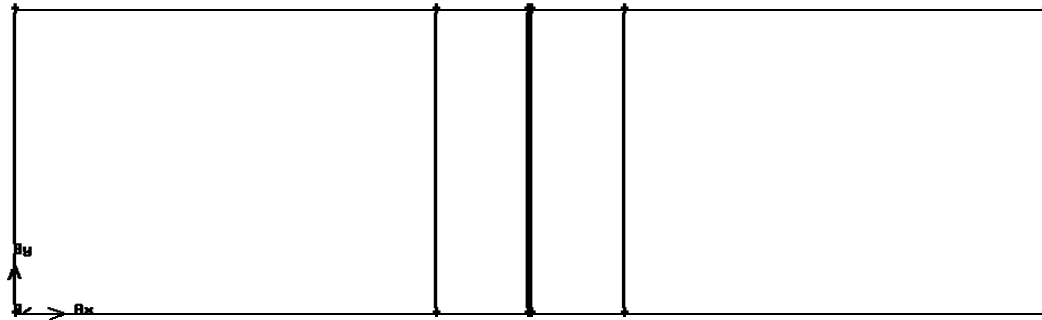
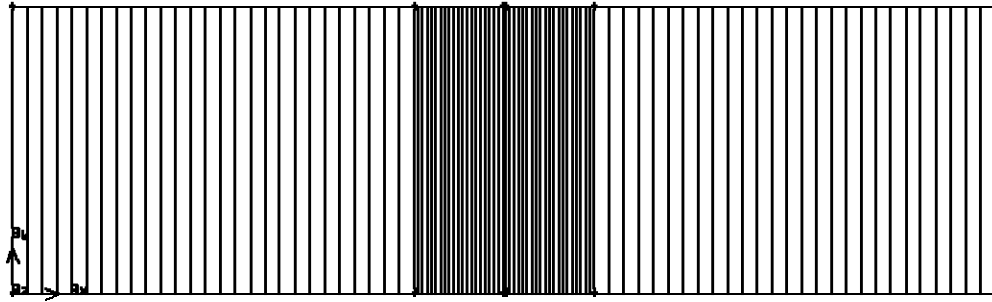


Figure 6.2 – GAMBIT MFC Model Wires

### 6.2.2 Mesh

The meshing is an important part of the geometry production, and it is the method GAMBIT divides the full geometry into smaller cells. The higher resolution the cells have, the better quality the solutions that are produced will have. However, larger number of cells will require the model longer computational time for a solution to converge. In order to balance both quality and computational time, it is possible to mix the resolution of cells so that areas of importance to the model that need high resolution, can have higher cell resolution than other less important parts of the geometry.

In the MFC model that has been constructed there are three different types of zones, which are anode/ cathode chamber, electrodes and the membrane. The chambers are assumed to have a fairly constant concentration, and are not of significant interest in the model, and therefore require only low resolution. The electrodes are of particular interest, and should therefore have a high resolution. The same goes for the membrane, which needs an extra high cell resolution since it divides two different parts of the fuel cell, and is very thin. Therefore, it was decided on having 27 cells in each chamber, which means 1 cell per mm. The electrodes needed 20 cells, or around 3.3 cells per mm. The membrane was decided to have 10 cells, which theoretically would mean 56 cells per mm. For details, see Figure 6.3.



**Figure 6.3 – GAMBIT MFC Model Meshing**

### **6.2.3 Zone Settings**

Finally, the last part that needs to be organized in GAMBIT, is to define the various zones. Previously, there has been made one face for each different element in the MFC. The zones are divided into two different types of zones; *boundary* and *continuum*.

The boundary types refers to walls, and axis of symmetry, or other edges in our model. The ones that are important to declare are left anode wall (anode\_end), right cathode wall (cathode\_end), the lower edge is declared as an axis for symmetry, and the top edges are declared as wall boundaries.

The second type that is needed to declare, are the *continuum* zones. This is done so that the faces can be declared to be made of either a fluid or a solid. In the MFC model, all the 5 elements present are assumed to be fluids, and only needed to be declared with suitable names (membrane, cathode\_electrode, cathode\_chamber, anode\_electrode, anode\_chamber).

The geometry was then exported by using the GAMBIT Export Mesh function, and selecting 2D mesh (mcf\_model.msh).

## 6.2.4 Importing the mesh into FLUENT

When opening up FLUENT, it is important to select the 2ddp version. This version takes into account that the geometry being modeled should be circulated around a symmetry axis, and is cylindrical in its solution form.

After opening up the right FLUENT version, the 2D mesh can be imported by selecting “open case” and choosing `mfc_model.msh`. The first thing that required attention was to change the scale of the MFC model, so that FLUENT knew the model was designed in mm and not meters which is the default. This was done in the *Grid* menu, under *Scale*.

## 6.3 Settings

### 6.3.1 Solver Settings

Once the mesh is imported, the next step was to define all the required settings. This was done through *Define > Models > Solver*. The only variable that needs to be change is adjusting the *Space* to *Axisymmetric*, so that FLUENT knows that the model is cylindrical (see Figure 6.4). Note that the solver was kept on the *Steady State* solver under the Time selections, even though the real MFC in lab experiments function in Unsteady (or transient) mode. This is because it is easier to analyze data in Steady State.

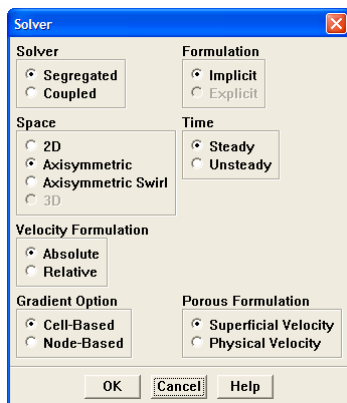
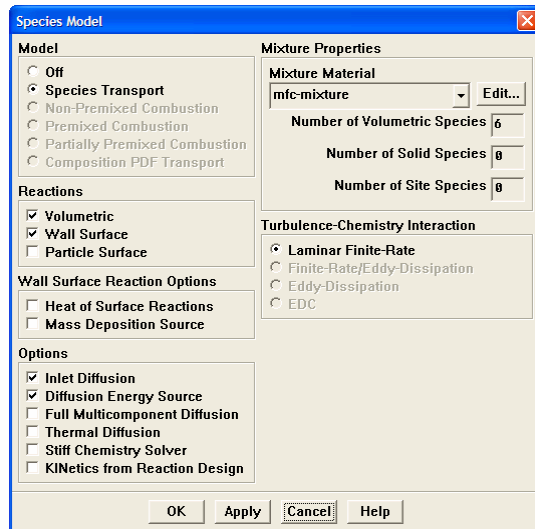


Figure 6.4 – FLUENT Solver Menu

Next step was to allow for more complex species models. This was done through *Define > Models > Species > Transport & Reaction*, and the user needed to activate *Species Transport*, together with *Volumetric* and *Wall Surface* reactions (see Figure 6.5).



**Figure 6.5 - FLUENT Species Model Menu**

After these general settings were completed, the materials needed to be created. All materials are originally created through the *Define > Materials* menu. From this menu all the new species were created, using the species details from Section XX in this thesis (see example Figure 6.6).

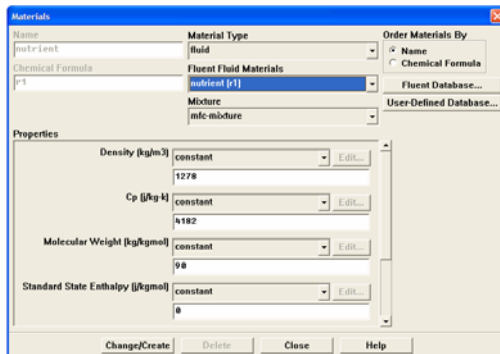


**Figure 6.6 - FLUENT Materials Menu**

In the same *Materials* menu, the various selected species was selected to be included in a *mixture* called *mfc-mixture*. There were two important factors, the first adding



the solution species (S) to the *Selected Species* list last (Figure 6.7 b), since the last selected species acts as the bulk species in the mixture. The second important change is to select the *volume-weighted-mixing-law* under the density (see box in Figure 6.7 a). The standard density method for FLUENT is by assuming ideal gas, but since the MFC is dealing with liquids, this would lead to incorrect calculations (see appendix).

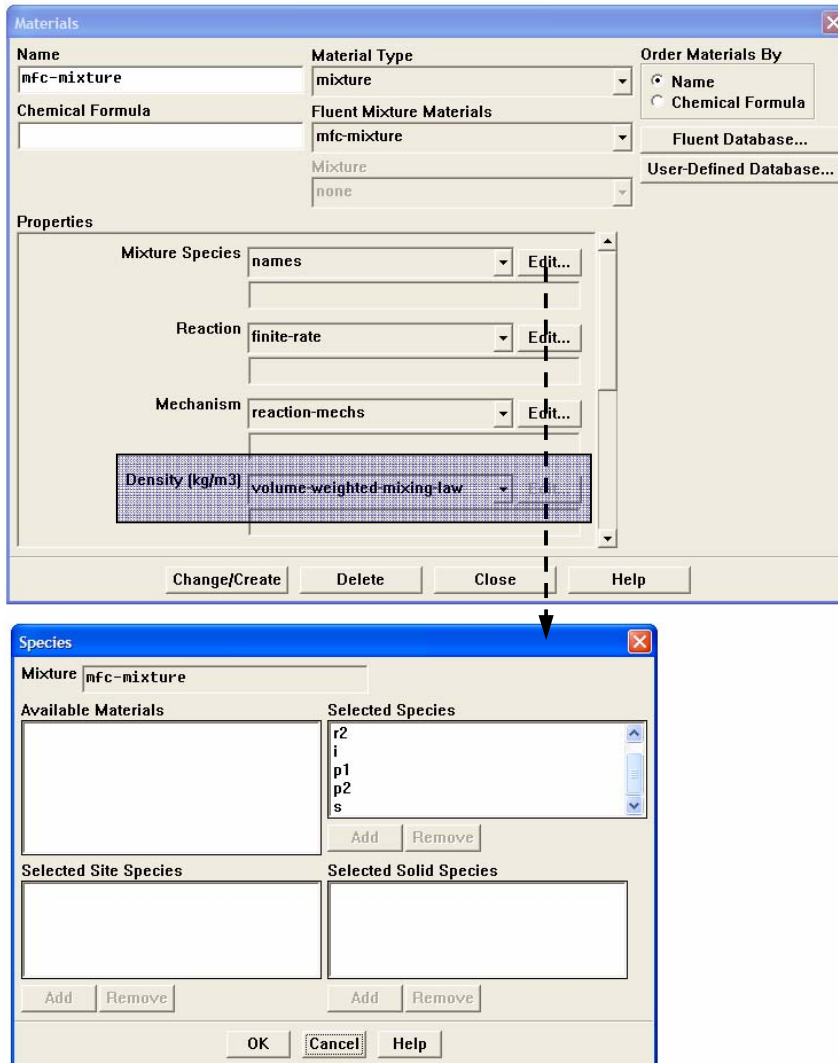


**Figure 6.7 a&b - FLUENT Material Mixture and Species**

Subsequently, the reactions and reaction mechanisms needed to be implemented through their respective menus under *Materials* (Figure 6.7 a&b). The reactions were taken from section 5.2 in this master thesis, and the two reaction mechanisms that are required are one for the anode and one for the cathode (and then eventually an alternative anode mechanism that includes the oxygen crossover effect).

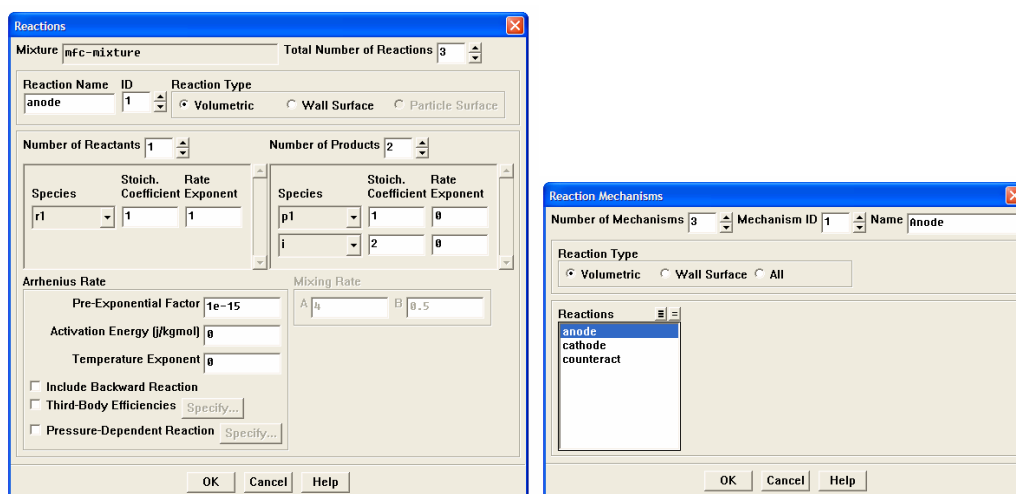


**Figure 6.8 a&b - FLUENT Reactions and Mechanisms**

Finally, it was important to set the *Diffusivity* of the mixture, which is also set in the *Materials* menu. However, in most of the models this was done by an UDF, and will be discussed in a later section.

In order to simplify the construction of a new model and testing of multiple geometries, the species, mixture properties and reaction mechanism data can be stored in a User-Defined Database. The data is stored in a single step by copying already configured data into a new User-Defined Database, and storing the file as name.scm. A copy of the User-Defined Database file produced for this MFC model (mfc.scm) can be found in appendix.

### 6.3.2 Boundary conditions

Next, it was important to set the correct boundary conditions for the model. The various boundary conditions, and what effect they have on the model, will be discussed. There are three types of boundary types that are used in this MFC model, which are *fluid* for the volumes and *wall* or *axis* for the edges.

For the fluids in the system, the only factor that needed changing was the *reactions*. All the 5 different fluid zones were opened up, and it was controlled that all except the anode and cathode electrodes had the reaction function turned off. In the anode

electrode the *anodic reaction mechanism* was chosen, and likewise in the cathode electrode.

It was assumed that there is no particular heat energy being released when the bacteria decompose the nutrient, or in any other part of the MFC. Because of this, it was assumed that the system is isothermal. In order for FLUENT to have a base temperature to adjust after, all the *wall temperatures* in the model were set at a fixed wall temperature of 300K (~room temperature). The axis, or centerline, does not have any required or possible settings.

There are various ways to control the species concentrations in FLUENT, either by a set mass fraction or by a no flux boundary. Often, a model needs to use a combination of these alternatives. The settings that were chosen for the MFC model (see Table 6.1), were nutrient and oxygen being held at a constant concentration at the anode and cathode end respectively, H<sup>-</sup> ions having a no flux boundary at all walls, and it was decided to drain the two products/waste species at both sides. Constant supply was done by setting a fixed mass fraction of the species at the end walls, while drains for specific species was implemented by setting the mass fraction of a species at the same wall to be zero. For the solution (S), or bulk species, it is not possible to set any boundary condition, since it is calculated solely by FLUENT.

**Table 6.1 - Boundary conditions for MFC model**

Species	Anode	Cathode
R1	Constant mass fraction	Drain
R2	Drain	Constant mass fraction
I	No flux	No flux
P1 & P2	Drain	Drain
S	n/a	n/a

## **6.4 User Defined Functions**

### **6.4.1 FLUENT and UDF**

FLUENT allows the use of User Defined Functions (UDF), which are C++ codes that can be run together with the FLUENT model. Not only can these UDFs alter almost any property in the model, but it has the ability to read properties, analyze their value, and then decide the appropriate value for properties that are dependent on the current state.

There are two ways of implementing UDF files into FLUENT, either by *interpreting* or *compiling* the file. In general, *interpreting* is an easy way of implementing small and simple UDF files. However, this is a process that occurs at run time, does not allow all C++ commands, and may make the system run unnecessarily slow. However, if the UDF files are *compiled*, they are translated by an external C++ compiler into the same language that FLUENT itself is run in. It allows a wider spectrum of C++ commands and will lead the simulations to run faster. More differences between these two will be discussed below.

In order to compile a UDF function the system needs to have a C++ compiler installed. The compiler selected for this research was Microsoft Visual C++ 2005 Express Edition<sup>25</sup>, a free version of Microsofts Visual Studio packages. The UDF code can essentially be written in any text editor, but since Visual C++ allows easy editing of the UDF files by color coding the commands, it has also been the preferred editing software.

A multitude of UDF files were tested during the construction of the MFC model. Two versions will be discussed, one *interpreted* and one *compiled*. Both the UDF files were implemented in such a way that they were called up for every iteration FLUENT took, and ran through every cell of the model. This meant the simulation took longer time, but the diffusivities were kept as accurate as possible.

### **6.4.2 Applying Diffusivities by use of UDF**

#### **Interpreted UDF**

The first version of the UDF was *interpreted*, and not compiled. In regards to this research work, the main difference between the compiled and the interpreted implementation was the amount of information the UDF file could extract from the model. The interpreted files could not extract the `thread_id`, which is external information about the cell referring to which zone the cell is located in (e.g. cathode, anode or membrane). Therefore, the interpreted UDF needed to use internal cell information, for example temperature. The solution was to set up a small temperature differences between each zone by applying specific wall surface temperatures ranging from 299 K and up to 301 K. From this it was possible to modify the diffusion coefficients fairly accurately between the zones. However, it was not a tidy solution, and the first version only allowed *constant dilute approximation* diffusivity, which only allow a common diffusivity to be set for the total mixture for each zone/temperature interval.

**Table 6.2 - Interpreted UDF Diffusivity Settings**

<b>Zone</b>	<b>Zone 1</b>	<b>Zone 2</b>	<b>Zone 3</b>
<b>Mixture</b>	D <sub>1</sub>	D <sub>2</sub>	D <sub>3</sub>

### **Compiled UDF**

The final UDF was *compiled*, which simplified the diffusivity process drastically. Not only did it have the ability to attain the `thread_id`, or location information for the cell it was working on. It also allowed the UDF to use the *approximate dilute* diffusion, which together with species id numbers could set specific diffusivities for each species individually in every zone in the fuel cell.

A copy of this UDF can be found in appendix. The UDF can easily be modified for different species diffusivities, a different turbulent diffusivity, or for a completely different MFC geometry. When changing the MFC geometry the zone id numbers and species id numbers would require checking before implementation, in addition to the various diffusivities being updated.

**Table 6.3 - Compiled UDF Diffusivity Settings**

<b>Zone</b>	<b>Zone 1</b>	<b>Zone 2</b>	<b>Zone 3</b>
<b>Species a</b>	D <sub>a.1</sub>	D <sub>a.2</sub>	D <sub>a.3</sub>
<b>Species b</b>	D <sub>b.1</sub>	D <sub>b.2</sub>	D <sub>b.3</sub>
<b>Species c</b>	D <sub>c.1</sub>	D <sub>c.2</sub>	D <sub>c.3</sub>

### **6.4.3 Future UDF possibilities**

UDF is a powerful tool to implement special functionality in a computational model. An improved UDF could take into account electrical forces and the electrical system. By measuring the concentration difference of charged ions between the anode and cathode chamber it is possible to implement electrical driven forces to make the mass transfer through the membrane more accurate. By the use of the UDF it is also very easy to implement drains or sources at specific locations in the fuel cell, with specific conditions of what they should do. This way, it is possible to allow electrons to be subtracted at the anode electrode and inserted into the cathode electrode at any given rate, which can be dependent on the load or resistance that is present at any given time.

## **6.5 Running the Model**

### **6.5.1 Iterations**

Since FLUENT uses numerical computations, an initial guess must be supplied before running a simulation. The closer this guess is to the actual solution, the easier and quicker it is for FLUENT to get the solution to converge. A converged solution is attained once the residual of all species fall under their convergence criteria, which means they are changing less than a certain fraction of its own value per new iteration. The residual that has been used most widely in the MFC model, has been 1e-08, which should provide a good steady state result.

In order to get the solution to converge as easily as possible, it was advantageous to use the previously iterated and converged data as the initialization data for the subsequent new simulation.

The settings for the steady state iterations are sparse, and the only two settings that needed to be changed were the number of iterations and the reporting interval. By increasing the reporting interval from the standard which is 1, and up to 1000, the speed increased drastically (see picture XX).

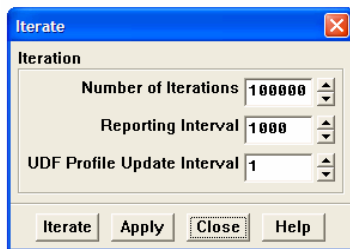


Figure 6.9 - FLUENT Iterations

## 6.5.2 Schemes

Once the model was working successfully, the goal was to attain multiple variable tests. These runs can be very time consuming if the user is required to manually enter the new values for the variables very time the simulation has converged. However, FLUENT allows users to upload schemes, which are instructions for FLUENT explaining step by step what to do. This made it possible for the user to run through a set of simulations in FLUENT with reaction rates varying from an order of  $1e-15$  and up to  $1e-3$ , without the user having to be present.

The schemes were also set to save the data, export the reaction rates, and could be used to store pictures of various graphs from the model (more about the storing of data in the next section). For an example of a FLUENT Scheme see Appendix XX.

## 6.5.3 Storing

Once the simulation has managed to converge, the data was stored for later use. There were three main files that needed to be saved from each experiment:

Case	Needed if the case (incl. reaction rate and settings) was to be reopened
Data	All cell information including species concentrations and other properties
Reactions	Reaction rates were exported in ASCII format simplifying analysis

Each of the three files was saved with the same file name, but different extensions (.cas, .dat and .txt). The filenames represented the essential information that had been tested in that specific simulation, which meant that a simulation testing forward reaction rates of  $1e-4$  and  $1e+5$  for the anode and cathode electrode respectively could be called;

*A1e-4\_C1e+5\_property1\_property\_2\_computerinfo.cas*

This method of naming files made it easier to look through and control the data.

## **6.6 Excel Analysis**

As previously stated, most of the electrical calculations were conducted externally to FLUENT. The main information that was needed from FLUENT was the reaction rates from the anode and cathode side. By comparing these two values, it was possible to check that the simulation had really achieved a steady state. If it is at a steady state, the two reaction rates divided by their own personal  $Z_i$  should be equal to each other ( $Z_i$  is 2 on the cathode side, and may be 2, 3 or 4 on the anode side). By using the cathodic reaction rate it is possible to find out how many electrons necessarily must have been passed through the electrical system, and thereby find the short circuit current of the MFC.

In order to simplify the Excel analysis, a standard formula sheet was made, making it easy for the user to copy and paste in the ASCII result file. The equations for the short circuit current were taken from section 0 in this master thesis. The reaction and current data was then put in a common table, where values could be more easily compared and analyzed.



## 7 Tests and Results from Computational MFC Model

### 7.1 Finding Appropriate Reaction Rates

The first task for the computational model was to find the appropriate reaction rate for the anode bacteria reaction. This was done by testing reaction rates in the model, and comparing the result to the Short Circuit Current (SCC) measured experimentally. The goal is to configure the model by finding the right reaction rate, so that the model thereafter can be used to make predictions. Based on the power estimations (see section 5.6) and experimental data the SCC has been calculated to be  $67.9 \mu\text{A}/\text{cm}^2$ .

The process was started by selecting an initial reaction rate for the anode reaction, testing it to see what the estimated current became, and then change the rate accordingly. Various anode reaction rates were tested, starting at reactions as low as  $1\text{e-}10$ .

At an anode reaction rate of  $1\text{e-}6$ , the concentrations of both nutrient and oxygen can be seen to decrease in the electrodes closer to membrane (see Figure 7.1 a&b).

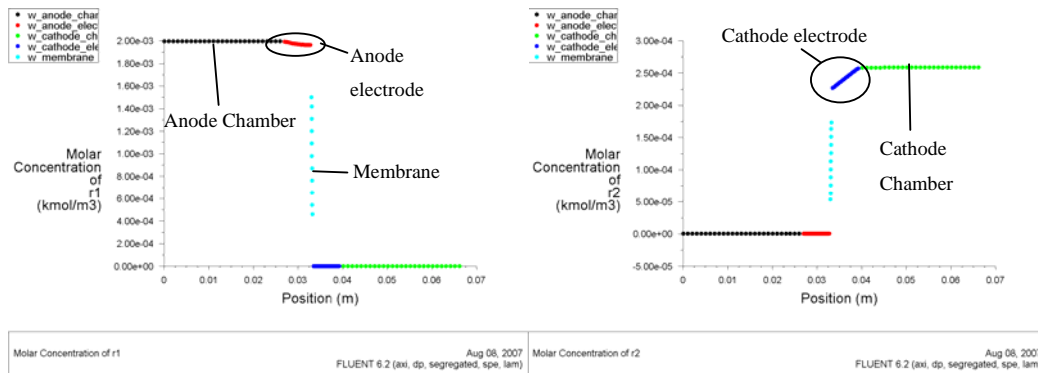
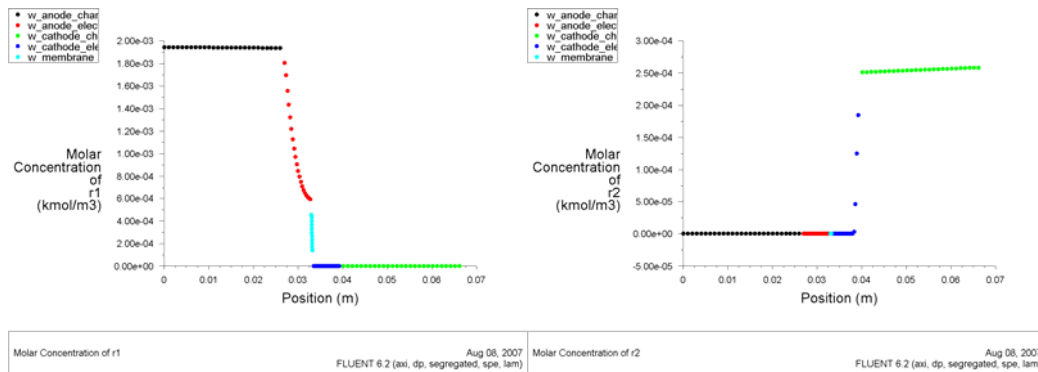


Figure 7.1 a&b – Nutrient and Oxygen Concentrations, Anode reaction rate:  $1\text{e-}6$

When increasing the anode reaction rate, concentration of intermediate ( $\text{H}^+$  ions) increases, which leads to a higher flux of  $\text{H}^+$  through the membrane. This again means a higher reaction at the cathode electrode, but also a higher current. The Excel

calculations gave an estimated current of only  $0.46\mu\text{A}/\text{cm}^2$  for this reaction rate, which means the rate needed to be increased.

As the anode reaction rate is increased, it is seen that the estimated current rises. However, when looking at the concentrations, it is apparent that already at an anode reaction rate of  $1\text{e-}4$  the oxygen is nearly completely consumed from inside the cathode electrode (see Figure 7.2 b). This leads to the idea that there might be an oxygen limiting factor on the anode side if the anode reaction rate is increased to much. The anode reaction rate shown below gave an estimated current of  $22.4\mu\text{A}/\text{cm}^2$ , which means it still needs to be increased.



**Figure 7.2 a&b - Nutrient and Oxygen Concentrations for Anode reaction rate:  $1\text{e-}4$**

Plotting the current that is achieved for each anode reaction rate on a graph, shows an unexpected behavior (see Figure 7.3). It shows that the current increases as the anode reaction rate increases, but somewhere between reaction rate  $1\text{e-}3$  and  $1.1\text{e-}3$  the current drops drastically. An investigation into the reason to why it decreased concluded that the transport of oxygen from the turbulent cathode chamber into the laminar cathode electrode was too small. If there is not enough oxygen in the cathode electrode to react with the amount of  $\text{H}^+$  ions coming through the membrane, there would become a buildup of  $\text{H}^+$  ions. It would seem that when the anode reaction rate was increased, it resulted in the model becoming unstable, and finally stabilizing again at around  $17\mu\text{A}/\text{cm}^2$  with an incredibly high  $\text{H}^+$  concentration

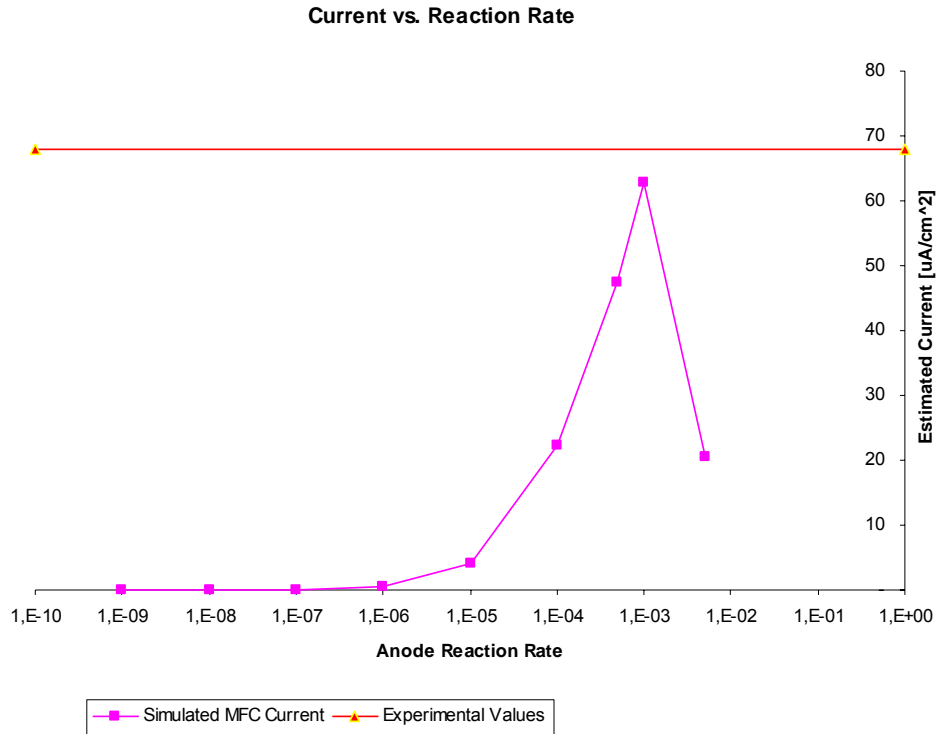


**Figure 7.3 - Estimated Current for MFC - With oxygen limitation**

To check this diagnosis and to try and find a solution for the problem the diffusivity of oxygen was increased gradually simultaneously with testing the different reaction rates. This showed that for low reaction rates there was no change at all to the estimated current if the diffusion rate of oxygen was increased. However, at higher reaction rates where the “regular” diffusivity dropped of, the simulations with higher oxygen diffusivity allowed the current to continue and increase (see Figure 7.4).

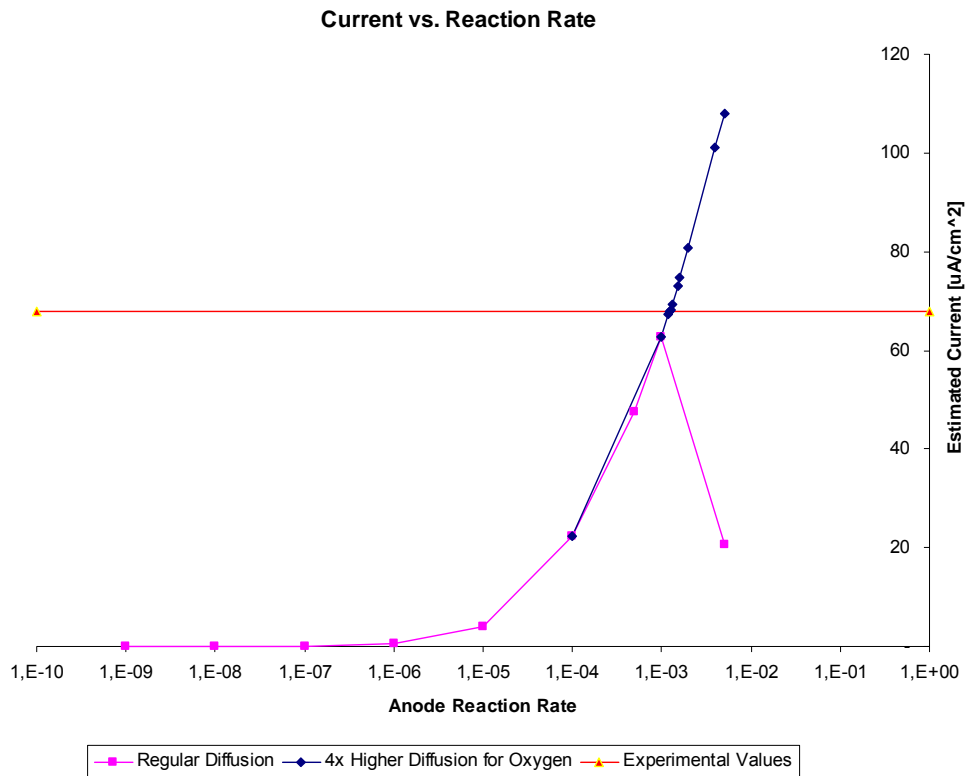


**Figure 7.4 - Finding required reaction rate**

When increasing the oxygen diffusivity into a 4x higher diffusivity, it is possible to achieve the types of currents that are required. From the results it is found that the appropriate reaction rate for the bacteria anode reaction rate is

$$k_1 = 1.23e-3$$

**7-I**

The tests also suggested that the transport of oxygen can be a possible limiting factor for the fuel cell that should be investigated more thoroughly.

## 7.2 Varying oxygen concentrations

The results from the initial test where the appropriate reaction rate for the anode reaction was found led to the idea that the system might have a limiting factor with regards to the oxygen transportation into the cathode electrode. The mass transportation of oxygen into the electrode is the result of multiple factors, the two main ones being concentration gradient and diffusivity coefficient.

When the diffusivity of oxygen was increased in previous examples, it was only shown to have an effect on the result of the very high reaction rates, which are where the regular diffusion rates had a large drop in estimated current. This test is to show what effect the oxygen concentration has on the current production.

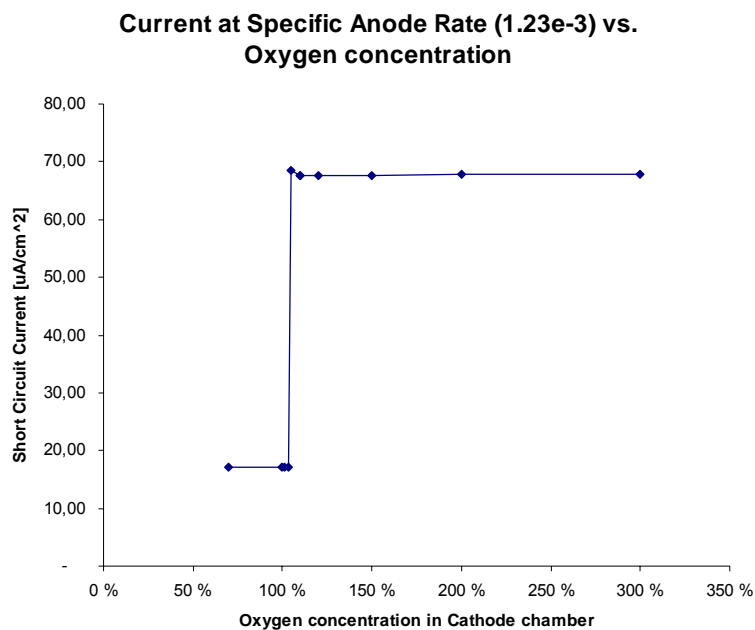


**Figure 7.5 - Current Depending on Oxygen Concentration**

Figure 7.5 shows estimated current as a function of the oxygen concentration ranging between 70% - 300% compared to the oxygen concentration originally calculated. The same anode reaction rate as was found earlier is used for the simulation. It is strangely noticeable that most of the results are completely constant, apart from at one point where it drops vertically.

From this data it was ascertained that there is an oxygen transportation limitation in the MFC model. However, as long as the required oxygen is lower than the oxygen that can be transported into the electrode, the oxygen concentration has no direct effect on the current production, i.e. it is not rate limiting. However, if the reaction mechanisms require more oxygen than the model manages to transport, the model will become unsteady.

### 7.3 Turbulence

Initially, there were done some tests without any turbulence in the anode and cathode chamber. However, it was found out at a very early stage in the research that the mass transportation of both nutrient and oxygen would strongly limit the current production for the MFC model if there was only laminar diffusion in the chambers. That is why the turbulent mixing caused by the air and nitrogen bubbles was taken into account.

This simulation was prepared in order to investigate how much the turbulent mixing effects the current production, trying to see whether the gasses that are bubbling in the chambers are necessary not only to purge the solution but maybe to mix as well.

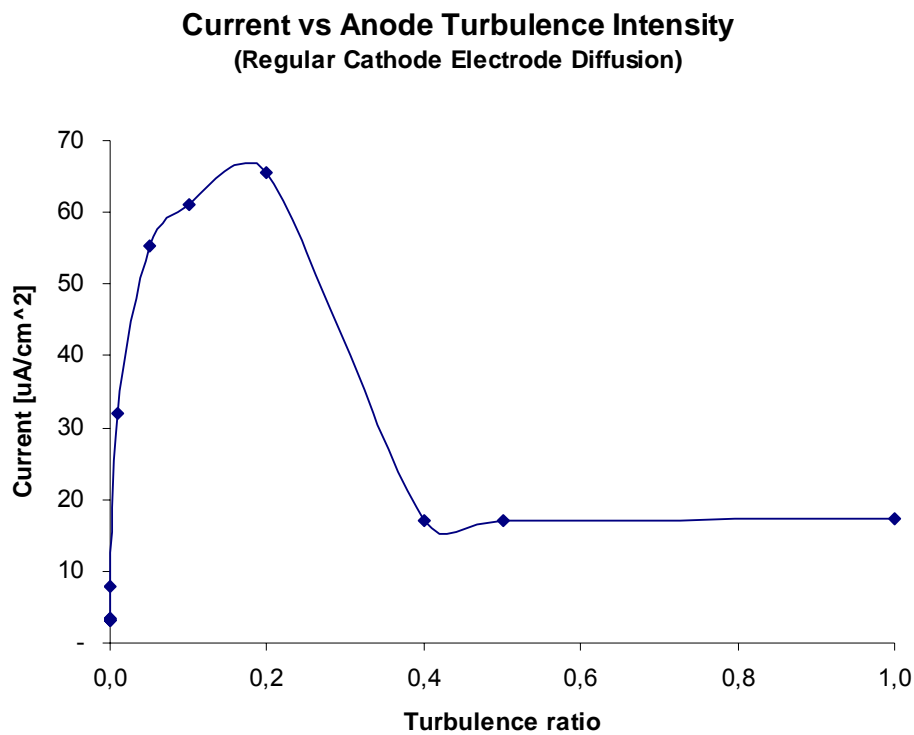


**Figure 7.6 - Current as a function of turbulence intensity in anode chamber**

As seen in Figure 7.6, nearly the whole increase in current that is achieved from the turbulence mixing is achieved already at a 0.1 fraction of the turbulence level calculated from gas bubbles. Again, there is a sharp decrease in the current as the anode activity increases over threshold of what the transportation of oxygen can

withstand. However, judging from the curve in the beginning of the graph, it seems as though even if the transportation of oxygen had not been a limiting factor, the increase in current due to an increase of turbulent mixing at any extent would max out soon after 0.2.

This means however, that if you have transportation in either chamber in the fuel cell that is controlled purely by laminar diffusion, even the slightest sign of turbulence would make a large impact in the current production. However, if turbulence already exists in the chamber, the addition of more turbulent sources would not manage to increase the current significantly.



#### ***7.4 Oxygen crossover from cathode to anode***

A problem in all fuel cells has been the crossover through the membrane of other species in addition to the H<sup>+</sup> ions that are intended to go through. In a regular fuel cell the problem can be either fuel permeating through and contaminating the cathode electrode, or oxygen coming through to the anode side reacting directly with the fuel without producing electricity.

In the case of MFCs, the nutrient consists of such a large molecular structure with a high molecular weight that it is believed it cannot permeate through the membrane. Oxygen however, is free to permeate from the cathode side through to the anode side. Once the oxygen reaches the anode side, the bacteria will utilize the oxygen in stead of using the electrodes, which means a loss of energy.

For these simulations the UDF was altered so that it allowed for oxygen diffusivity in the membrane. The reaction rate for the counteracting reaction was enabled and set at  $k_3=1e+5$ , which is a fast reaction.

**Current lost due to oxygen cross over at various reaction rates  
Regular Diffusion at Cathode Electrode**

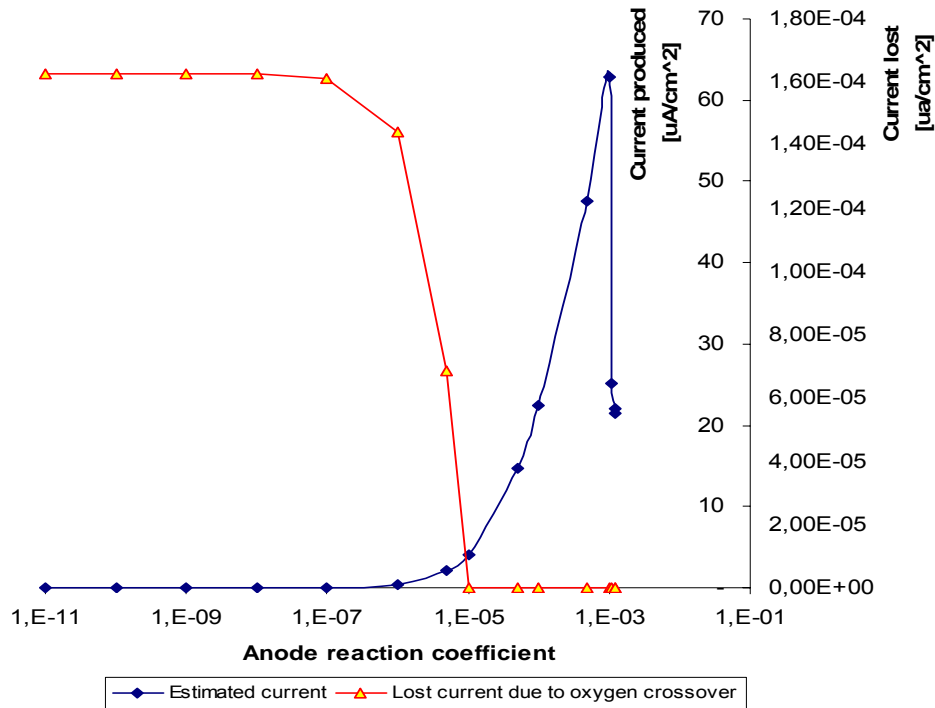


**Figure 7.7 - Crossover effect of oxygen**

The first obvious detail, is that the lost current (lost energy) due to oxygen crossover through the membrane, is around 5 orders of magnitude lower than the maximum produced current. The result is presented in Figure 7.7, where it is important to notice the double y-axis with different units. It can be seen that for an increasing anode reaction rate, the produced current increases, while the lost current starts to drastically decrease. This is the result of the oxygen being completely consumed on the cathode by the released H<sup>+</sup> ions which comes when the anode reaction rate is increased. At very low reaction rates however, between 1e-10 and 1e-9 the two currents (lost and produced) are of comparable sizes.

## 7.5 Diffusion Calculations

Investigating the transportation limitation for oxygen from the cathode chamber and into the cathode electrode.

By using the equation for diffusivity and data from the MFC model, it was possible to investigate the oxygen transportation limitations. It was assumed constant concentration through the whole anode chamber, and only laminar diffusion inside the cathode electrode. The required current is still 67.9 uA/ cm<sup>2</sup>.

Diffusion is defined:

$$J_i = -D_i \frac{dC_i}{dx} \quad 7-II$$

Assuming a species is going towards a drain at point  $x$ , it can be written:

$$J_i = -D_i \frac{-C_i}{x} \quad 7-III$$

The current that is attained from this flux is found by:

$$\dot{I} = J_i * F * Z = D_i \frac{C_i}{x} * F * Z \quad 7-IV$$

Whereby the maximum possible diffusion distance can be found from:

$$x = D_i \frac{C_i}{\dot{I}} * F * Z \quad 7-V$$

The data from the MFC model states:

$$\begin{aligned} D_i &= 2.18e^{-9} m^2 / s & F &= 9.6485e^7 C / kmol \\ C_i &= 2.6e^{-4} kmol / m^3 & Z &= 2 \\ \dot{I} &= 67.9uA / cm^2 = 0.679A / m^2 \end{aligned}$$

Maximum distance the oxygen can diffuse in the quantity needed to supply the SCC measured in the experiments is found from:

$$\begin{aligned} x &= D_i \frac{C_i}{\dot{I}} * F * Z = 2.18e^{-9} m^2 / s * \frac{2.6e^{-4} kmol / m^3}{0.679A / m^2} * 9.6485e^7 C / kmol * 2 \\ x &= 8.05 * 10^{-5} m = 0.081mm \end{aligned}$$

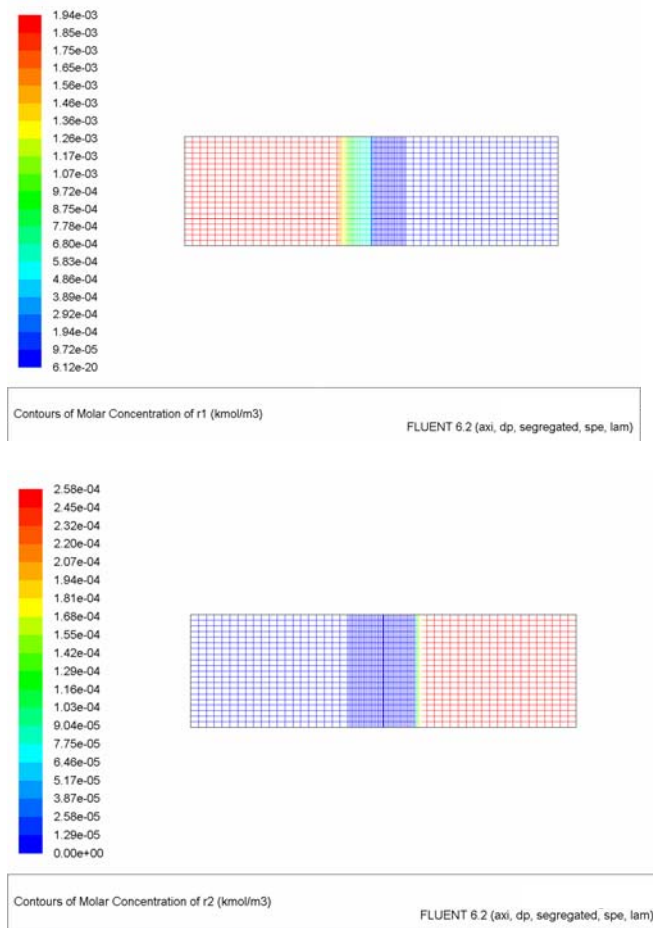

---

Mesh size for electrodes in MFC model: 6mm/20 = 0.3mm

## 7.6 Geometries 2D

In order to change the 1D FLUENT model into a 2D version, the mesh needs to be redone. This was done in GAMBIT, and reinserted into FLUENT. When running the iterations on the 2D version, the iteration took as expected longer time, but worked in the similar way as the 1D.

In the future it is now possible to construct advanced 2D models, and use the same FLUENT model to do the analyzes on the mesh.



## 8 Discussion

Probably the most noticeable result has been the transportation limitation of oxygen, which has affected all of the other results in some way or other. The first question to ask, is whether this transport limitation is real or whether it is purely a model error.

The Diffusion Calculations in section 7.5 tries to give an answer to this, which leads towards the only problem with the oxygen transportation is that the cell meshing in the cathode electrode is too large. Because the mesh size is 0.3mm, and not 0.08mm which would be required in order for FLUENT to manage to calculate maximal diffusion, the model becomes unstable and builds up the H<sup>+</sup> species. Therefore the direct answer to the question would be yes, the oxygen transportation limitation would go away if the mesh size was 0.08 mm thick.

However, the maximum diffusion distance of oxygen also corresponds to the distance for within where oxygen needs to be completely consumed by reactions in order to produce the required current production. This again, means that 100% of the reaction needs to take place in only 1% of the cathode electrode. If the cathodic reaction rate is too slow, a similar unsteadyness result would be expected. Since the cathode is coated with platinum however, it might be a fair assumption to state that all the oxygen would be consumed. This would mean that the limitation for the oxygen transportation is purely based on the meshing. However, the superficial oxygen transportation limit does lead to an interesting design question, which is why the cathode electrode takes up so much space (6mm) if a thin slice of 80um would give the same result?

When trying to find the anode reaction rate in section 7.1, it was decided to go around the oxygen limitation problem by increasing the diffusivity of oxygen in the cathode electrode until the limitation was gone. Since the results below the critical reaction rate with the high O<sub>2</sub> diffusivity proved identical to the ones with regular diffusivity, it was assumed that it was correct for the higher reaction rates too. Therefore, the forward reaction rate found in section 7.1 should be valid,  $k_1 = 1.23e-3$ .

Naturally, the simplifications done with respect to choice of reaction mechanisms, number of species and neglect of backward reaction rates, limits the accuracy of the reaction rate. However, as long as the variables are kept similar to the ones used in the calibration of the model, the rate can be used as a good indicator for what will happen.

One very interesting test was the anode turbulence simulations in section 7.3. The appealing factor is that a even slight increase in the mixing, given that the solution starts off close to laminar, could result in a great increase in power. This tendency is also supported well by empirical data (see section 3.2.3), which showed a large increase in power if stirring rods were initiated whilst no other mixing units were present, compared to only a minor increase when nitrogen already was bubbling through the chamber. Again, the results show oxygen to be transport limited when the turbulence reaches a certain magnitude, which seems to be a weakness in the model. The turbulent mixing should definitely be taken into account when designing a MFC, since it may be a very cost effective and space efficient way to increase the power.

Yet another interesting area in the simulation was the oxygen crossover. If given the knowledge that oxygen already is transport limited, it was not surprising to see that the simulated results showed no current loss at high rates. However, the fact that the maximum crossover effect when close to no current was produced by the cell only reached a low  $1.8 \cdot 10^{-4}$  uA/cm<sup>2</sup>, was surprising. It even leads to think of other factors such as if the diffusion of O<sub>2</sub> in the Nafion membrane could be too low, or that there might be external pressure differences acting on CFC system that encourages higher diffusion. It would be interesting to see what the effect would be if the diffusion in the membrane was more similar to the one of water.

The fact that the model has been using traditional diffusion-reaction mechanisms to model a biological fuel cell has so far proved to work very well. However, since the bacteria are live species, the experimental data in the lab often show large variations. The simulated model in FLUENT however does not at the moment not have a way of taking into account these dynamic properties of the bacteria, and whether the bacteria is becoming stronger or weaker.

There are still a lot of properties that still needs to be included in the model, where one of the more important ones would be the electrical driving forces. Also, implementing a function in FLUENT that make it is possible to show the estimated Short Circuit Current for a given model would result in a large simplification in use.

Implementing the 2D models works exactly the same way as the 1D models, but do take longer time. The 2D models make it possible to make test more advanced geometries for the fuel cell.

## 9 Conclusion

The first MFC model, described in the above analysis, has been validated as a model yielding accurate results through its highly correlation with lab tested empirical data. The most successful tests were the turbulence simulation (section 7.3) and oxygen crossover simulation (section 7.4). Both of these simulations can be used to predict valuable energy outputs.

Using diffusion-reaction mechanisms to model a biological fuel cell has proved to work well, though the model at the moment lacks some of the diversity and possibly arbitrariness that bacteria possess.

While there are still many properties that remain to be included in the model, such as electrical driving forces, the model has accomplished its objective and marks the first step towards a fully functional computational MFC model.

The MFC modeling is part of a 5 year program, and the model is therefore still being worked on. The next steps that are planned to perform are:

1. Advanced 2D models, including finned membrane
2. Electrical driving forces
3. More exact reaction kinetics, look at waste
4. Take into account more variables:
  - a. Temperature
  - b. Bacteria type
  - c. Transient analysis



## 10 Bibliography

### Empirical references:

#### Case 1:

A. Erten, L. Iverson, P. Ronney, Experimental MFC Data, 2007, University of Southern California (unpublished)

#### Case 2:

O. Bretschger, K. Nealsen, Experimental MFC Data, 2007, University of Southern California (unpublished)

### Literature references:

<sup>1</sup> Introduction: The immense potential of MFCs [online]

<http://mfc-muri.usc.edu/overview/intro.htm>

[Accessed 6 Jul 2007]

<sup>2</sup> Kenneth Nealsen, 2006, Microbial Fuel Cells (MFCs): Biofuels for Energy Production and Waste Disposal

Provost's Energy Retreat FEEI, February 24 -25, 2006

<sup>3</sup> About Shewanella oneidensis [online]

<http://mfc-muri.usc.edu/public/about.htm>

[Accessed 6 Jul 2007]

<sup>4</sup> Batteries and Fuel Cells

[http://www-scf.usc.edu/~chem115/scans/Ch12\\_fuelcells\\_notes.pdf](http://www-scf.usc.edu/~chem115/scans/Ch12_fuelcells_notes.pdf)

[Accessed 6 Jul 2007]

<sup>5</sup> Kenneth Nealsen, 2006, Making Electric Power with Microbes: Putting the Bio in BioFuelcells [online]

[http://mfc-muri.usc.edu/logon/forum/publications/electric\\_power.pdf](http://mfc-muri.usc.edu/logon/forum/publications/electric_power.pdf)

[Accessed 6 Jul 2007]

<sup>6</sup> Y. A. Gorby, S. Yanina, J.S. McLean, K. M. Rosso, D. Moyles, A. Dohnalkova, T.J. Beveridge, I.S. Chang, B.H. Kim, K.S. Kim, D.E. Culley, S.B. Reed\*, M.F. Romine, D.A. Saffarini\_, E.A. Hill, L. Shi, D.A. Elias, D.W. Kennedy, G. Pinchuk\*, K. Watanabe, S. Ishii, B. Logan, K.H. Nealsen, and J.K. Fredrickson, Electrically conductive bacterial nanowires produced by Shewanella oneidensis strain MR-1 and other microorganisms

<http://www.pnas.org/cgi/reprint/103/30/11358.pdf?ck=nck> [online, accessed 6 Jul 2007]

<sup>7</sup> O. Bretschger, S. Finkel, L. Iverson, B. Kim, F. Manfeld, K. Nealsen, S. Prakash, P. Ronney, H. Wanh, A. Lüttge, Bioengineered Fuel Cells: Optimization via Genetic Approaches and Multi-Scale Modeling, (Published), 2006

- <sup>8</sup> R. O'Hayre, S-W. Cha, W. Colella, F.B. Prinz, *Fuel Cell Fundamentals*. John Wiley & Sons, New York, 2006
- <sup>9</sup> General Modeling Specifications [online]  
[http://www.fluent.com/software/fluent/modeling\\_spec.htm](http://www.fluent.com/software/fluent/modeling_spec.htm)  
[Accessed 6 Jul 2007]
- <sup>10</sup> Fluent 6.3 Users Guide – (20.1-35) [online]  
<http://www.fluent.com/software/fluent/index.htm>  
[accessed July 6 2007]
- <sup>11</sup> Fluent 6.3 Users Guide – (8.3-7) [online]  
<http://www.fluent.com/software/fluent/index.htm>  
[accessed July 6 2007]
- <sup>12</sup> R. O'Hayre, S-W. Cha, W. Colella, F.B. Prinz, *Fuel Cell Fundamentals*. John Wiley & Sons, New York, 2006  
Fuel Cell Charge Transport
- <sup>13</sup> R. O'Hayre, S-W. Cha, W. Colella, F.B. Prinz, *Fuel Cell Fundamentals*. John Wiley & Sons, New York, 2006  
Table 4.1, page 96
- <sup>14</sup> Fluent 6.3 Users Guide – (14.1-1) [online]  
<http://www.fluent.com/software/fluent/index.htm>  
[accessed July 6 2007]
- <sup>15</sup> G.L. Borman, K.W. Ragland, *Combustion Engineering*, p. 110, WCB/McGraw-Hill, 1998
- <sup>16</sup> G.L. Borman, K.W. Ragland, *Combustion Engineering*, p. 110, WCB/McGraw-Hill, 1998
- <sup>17</sup> Fluent 6.3 Users Guide – (14.1-10) [online]  
<http://www.fluent.com/software/fluent/index.htm>  
[accessed July 6 2007]
- <sup>18</sup> Fluent 6.3 Users Guide – (14.1-7) [online]  
<http://www.fluent.com/software/fluent/index.htm>  
[accessed July 6 2007]
- <sup>19</sup> [www.chemfinder.cambridgesoft.com/](http://www.chemfinder.cambridgesoft.com/)
- <sup>20</sup> Alper Erten – April 26th 2007
- <sup>21</sup> Examples of pH values  
<http://hyperphysics.phy-astr.gsu.edu/hbase/chemical/ph.html>  
[accessed 6 Jul 2007]
- <sup>22</sup> Chemical-Specific Data Deisting Technical Support, August 2000,

[http://www.epa.gov/earth1r6/6pd/rcra\\_c/pd-o/appd1a.pdf](http://www.epa.gov/earth1r6/6pd/rcra_c/pd-o/appd1a.pdf)

[accessed 6 Jul 2007]

<sup>23</sup> X. Zhou, Z. Chen, F. Delgado, D. Brenner, and R. Srivastava, Atomistic Simulation of Conduction and Diffusion Processes in Nafion Polymer Electrolyte and Experimental Validation, Journal Electrochemical Society 154, B82 (2007)

<sup>24</sup> S.S. Kocha, J.D. Yang, and J.S. Yi, Characterization of Gas Crossover and Its Implications in PEM Fuel Cells, UTC Fuel Cells, South Windsor, CT 06074

<sup>25</sup> Microsoft Visual Studio Express Edition [online],

<http://msdn.microsoft.com/vstudio/express/downloads/default.aspx>

[accessed 10 Aug 2007]

# 11 Appendices

## 11.1 Reality Checks

Throughout the master thesis research and the development of the model, reality checks have been performed on the results and values in the model. This is a way to control that the model is working as expected, and it gives a continuous feedback on how the model is progressing. A selection of the tests will be presented here.

### 11.1.1 Density check

An early reality check that was made on in the modeling was looking at the density of the total mixture. Since the bulk species of the mixture is assumed to be water, the density should naturally be around  $998 \text{ kg/ m}^3$ . However, when checking the density of the mixture it showed  $0.731 \text{ kg/ m}^3$ . This is much closer to what one would expect the density to be if the mixture was gas.

By finding this error, it was found that in order for FLUENT to calculate the density in a correct manner the user needs to change the density calculation method from the default *Ideal-gas-law* and into the *Volume-weighted-mixing-law*.

### 11.1.2 Bottle necks in diffusion transportation for the current production

In order to test the validity of the species concentrations, and the electrical system calculations, various reality checks were performed. By using diffusion theory, it was possible to find possible bottlenecks, and also verify whether the model is working correctly.

#### *Nutrient diffusion from the anode chamber into the anode electrode*

It is assumed that the turbulent mixing in the anode chamber is more than high enough for sufficient transport of nutrient from the anode end wall and through the main

chamber. In the electrode however, it is assumed there is only laminar diffusion, which is around two orders of magnitude lower than the turbulent diffusion. It is therefore possible to perform calculations on the diffusivity to check whether the diffusion rate is high enough to withstand the mass transportation needed to produce the short circuit current that is measured experimentally.

For the calculations it is assumed that the nutrient concentration in the anode chamber is held at a constant concentration. To make a worst case diffusion scenario, it is assumed that all the nutrient has to pass through the whole 6mm thick electrode, and that it only reacts right before the nutrient meets the membrane. On the other hand, it is assumed that the reaction at this point is infinitesimally fast, so that all nutrient is consumed acting as a sink.

The general formula for molar flux by diffusivity is given by:

$$J_i = -D_i \frac{dC_i}{dx}$$

Where  $D_i$  is the diffusivity of the species in the solution [ $m^2/s$ ], and  $\frac{dC_i}{dx}$  stands for the concentration gradient. For the calculations currently being performed, the concentration gradient will use the anode chamber concentration at the electrode entrance, and a 0 concentration at the electrode end (6 mm). Using these values, the maximum mole flux generated is:

$$J_i = -1.10e-09[m^2/s] * [m^2/10^4 cm^2] * \frac{-3.9e-3[kmol/m^3]}{0.006[m]} = 7.15 * 10^{-14} \left[ \frac{kmol}{s * cm^2} \right]$$

Using Faradays constant (F) of  $9.6485 * 10^7$  C/kmol, and also assuming every nutrient will liberate 2 electrons (Z) into the electrical circuit, the short circuit current production per projected surface area is found to be:

$$\dot{i} = J_i * F * Z = 7.15 * 10^{-14} \left[ \frac{kmol}{s * cm^2} \right] * 9.6485 * 10^7 \left[ \frac{C}{kmol} \right] * 2$$

$$\dot{i} = 0.0000138 \left[ \frac{A}{cm^2} \right] = 13.80 \mu A / cm^2$$

The current measured in experimental lab tests has been up to around 750uA, or 67.9 uA/ cm<sup>2</sup>. Since the current calculated above is smaller, the diffusion of nutrient can be a potential bottle neck. However, if the diffusion requirements are made less restricted taking into account that the nutrient can be consumed earlier on in the electrode, it is possible to find out how far the nutrient can diffuse given a certain reaction rate (i.e. current production). It is important to keep the units the same, so  $\dot{I}$  needs to be calculated into A/ m<sup>2</sup>, which gives  $67.9 \text{ uA/ cm}^2 = 67.9 * 10^{-6} * 10^4 = 0.679 \text{ A/ m}^2$ .

$$\dot{I} = J_i * F * Z = -D_i * \frac{dC_i}{dx} * F * Z = D_i * \frac{C_i}{x} * F * Z$$

$$\Downarrow$$

$$x = \frac{D_i * C_i * F * Z}{\dot{I}}$$

This gives:

$$x = \frac{D_i * C_i * F * Z}{\dot{I}} = \frac{1.1e-09[m^2 / s] * 3.9e-3[kmol / m^3] * 9.6485 * 10^7 [C / kmol] * 2}{0.679[A / m^2]}$$

$$x = 0.00061m = 0.61mm$$

This shows that the amount nutrient needed to be decomposed in order to achieve the maximum current at short circuit only can diffuse 0.61mm into the anode electrode by plain diffusion. This means that the nutrient will have to be decomposed by the bacteria in the first third of the electrode thickness. In the MFC FLUENT model this is made possible by increasing the reaction rate, however in real life the reaction rate will be more limited by the surface area available so the nutrient transportation could be a possible bottle neck in the fuel cell.

It can be mentioned that the fuel cell in the experiment has not been worked on a short circuit for an extended amount of time, and that the current needed normally is lower.

A possible design solution for this problem would be to decrease the thickness of the electrode so that the nutrient has less of a distance to diffuse, and a larger part of the reaction will then occur closer to the membrane.

***Oxygen diffusion from the cathode chamber into the cathode electrode***

The same calculations can be performed for the oxygen in the cathode chamber. First it is assumed that the concentration is constant in the cathode chamber, there is only laminar diffusion inside the cathode electrode, and all of the oxygen is consumed at the membrane wall. This gives the following maximum value for oxygen mole diffusion flux:

$$J_i = -D_i \frac{dC_i}{dx} = -2.18e-09 [m^2/s] * [m^2/10^4 cm^2] * \frac{-2.6e-4 [kmol/m^3]}{0.006 [m]}$$

$$J_i = 9.45 * 10^{-15} \left[ \frac{kmol}{s * cm^2} \right]$$

This again results in a current of:

$$\dot{i} = J_i * F * Z = 9.45 * 10^{-15} \left[ \frac{kmol}{s * cm^2} \right] * 9.6485 * 10^7 \left[ \frac{C}{kmol} \right] * 2$$

$$\dot{i} = 1.82 \mu A / cm^2$$

Again, by decreasing the restrictions, we can find the distance the oxygen can diffuse at the needed rate:

$$x = \frac{D_i * C_i * F * Z}{\dot{i}}$$

$$x = \frac{2.18e-09 [m^2/s] * 2.6e-4 [kmol/m^3] * 9.6485 * 10^7 [C/kmol] * 2}{0.679 [A/m^2]}$$

$$x = 1.61 * 10^{-4} m = 0.161 mm$$

In order for the mass flux of oxygen to be high enough, the reaction rate on the cathode side needs to be fast enough so that all the oxygen can be consumed within

the first 0.38 mm of the cathode electrode. Since the cathode electrode is coated with an aluminum catalyst, the reaction is considered to be very fast. Also, the air bubbling into the cathode chamber creating turbulent mixing in the chamber might be creating a slight turbulent mixing close to the electrode wall as well. This could result in an increase of the diffusivity of all species in the fractional part of the electrode closest to the chamber. This possibility is not taken into account in the current MFC model, and it is unclear how far into the electrode this potential turbulent diffusion layer would penetrate.

For reference, the electrodes in the MFC model is model with a 20 cell mesh, giving a cell width of 0.3mm. Therefore, the highest current that be produced before becoming oxygen transport limited by the diffusion, is:

$$\begin{aligned} \dot{i} &= J_i * F * Z = -D_i * \frac{dC_i}{dx} * F * Z \\ \dot{i} &= -2.18e-9 [m^2/s] * \frac{2.6e-4 [kmol/m^3] - 0}{0 - \frac{0.006m}{20}} * 9.6485 * 10^7 \left[ \frac{C}{kmol} \right] * 2 \\ \dot{i} &= 0.364 A/m^2 = 36.5 \mu A/cm^2 \end{aligned}$$

This would correspond to the maximum current that can be produced by the fuel cell model, without the H<sup>+</sup> ions building up in both the cathode and anode chamber from lack of oxygen.

### ***H<sup>+</sup> ion diffusion from the anode through the membrane and into the cathode***

Similarly, it is possible to find out to what extent the diffusion of H<sup>+</sup> ions can be a limiting factor for the MFC current production. The concentration of H<sup>+</sup>, or pH value, is not a fixed value, but the pH will need to be held within certain levels in order for the MFC to function properly.

For the maximum current measured in the experiments, it is possible to find the required H<sup>+</sup> concentration difference over the membrane to withstand the flux. This



can be done by altering the equation for the current flux used earlier. The Z for H<sup>+</sup> ions is 1, compared to 2 for oxygen and nutrient.

$$\begin{aligned} \dot{I} &= D_i * \frac{dC_i}{dx} * F * Z \\ \Downarrow \\ \Delta C_i &= \frac{\dot{I} * \Delta x}{D_i * F * Z} = \frac{0.679[A/m^2] * 177.8 * 10^{-6}[m]}{2.2 * 10^{-8}[m^2/s] * 9.6485 * 10^7[C/kmol] * 1} \\ \Delta C_i &= 5.7 * 10^{-5} \left[ \frac{kmol}{m^3} \right] \end{aligned}$$

If it is assumed that all the H<sup>+</sup> ions in the cathode chamber is consumed by the fast cathodic reaction, the concentration of H<sup>+</sup> ions needs to be a minimum of 5.7\*10<sup>-5</sup> [kmol/m<sup>3</sup>] in the anode chamber. The concentration established at an anode pre exponential factor of 1.5e-4 is around 1.3 \* 10<sup>-3</sup> [kmol/m<sup>3</sup>] in the anode chamber, and 1e<sup>-4</sup> [kmol/m<sup>3</sup>] in the cathode chamber. This gives a concentration difference of 1.2\*10<sup>-3</sup> [kmol/m<sup>3</sup>], which is more than sufficient to create the flux current needed, and could actually withstand a current of up to:

$$\begin{aligned} \dot{I} &= J_i * F * Z = -D_i * \frac{dC_i}{dx} * F * Z \\ \dot{I} &= -2.2e-8[m^2/s] * \frac{1.18e-3[kmol/m^3] - 0}{0 - 177.8 * 10^{-6}[m]} * 9.6485 * 10^7 \left[ \frac{C}{kmol} \right] * 1 \\ \dot{I} &= 14.1A/m^2 \end{aligned}$$

Therefore, the H<sup>+</sup> ion transportation through the membrane should not be a limiting factor for the flux current production in the MFC model.

## 11.2 Computer tools

### UDF File – 2<sup>nd</sup> generation

```
DEFINE_DIFFUSIVITY(mfc_no_oxi,c,t,i)
{
  /* Variables */
  int zone_id, a_chamber, c_chamber, a_electrode, c_electrode, membrane;
  int R1, R2, P1, P2, I, S;
  real d_m,spe_eff[20],spe_memb[20],diff,diff_turb;

  zone_id=THREAD_ID(t);

  /* Input variables that needs to be checked */
  a_chamber      = 6; /* anode chamber id */
  c_chamber      = 4; /* anode chamber id */
  a_electrode    = 5; /* anode and cathode electrode id */
  c_electrode    = 3; /* anode and cathode electrode id */
  membrane       = 2; /* membrane id */

  /* Species index */
  R1 = 0;
  R2 = 1;
  I  = 2;
  P1 = 3;
  P2 = 4;
  S  = 5;

  /* Species regular diffusion */
  spe_eff[R1]=1.1e-9;
  spe_eff[R2]=2.18e-9;
  spe_eff[I]=2.2e-8;
  spe_eff[P1]=1.1e-9;
  spe_eff[P2]=3.2e-9;
  spe_eff[S]=3.2e-9;

  /* Species membrane diffusion */
  spe_memb[R1]=1e-22; /* approx 0 */
  spe_memb[R2]=1e-22; /* approx 0 */
  /*spe_memb[R2]=0.6e-10; oxygen cross over */
  spe_memb[I]=5.0e-10;
  spe_memb[P1]=1e-22; /* approx 0 */
  spe_memb[P2]=1e-22; /* approx 0 */
  spe_memb[S]=1e-22; /* approx 0 */

  /* Turbulent diffusivity */
  diff_turb = 1.98E-6;

  /* Diffusivity calculations */
  if(zone_id==a_chamber) {
    d_m = spe_eff[i] + diff_turb;
  } else if(zone_id==c_chamber) {
    d_m = spe_eff[i] + diff_turb;
  } else if(zone_id==a_electrode) {
    d_m = spe_eff[i];
  } else if(zone_id==c_electrode) {
    d_m = spe_eff[i];
  } else if(zone_id==membrane) {
    d_m = spe_memb[i];
  } else {
    d_m = 0;
  }
  return d_m;
}
```

## 11.2.1 User-Defined Database

Partial printout of the database that was produced that stores mixture, species, reactions and reaction mechanism for the MFC model. The full version includes one section for every species, and one section describing the mixture properties and reactions. The full version of the database can be found in the selection of files submitted together with the thesis.

```

////////////////////////////////////
;;;
;;;          FLUENT USER DEFINED MATERIAL DATABASE          ;;;
;;;
;;; (name type[fluid/solid] (chemical-formula . formula)    ;;;
;;;          (prop1 (method1a . data1a) (method1b . data1b)) ;;;
;;;          (prop2 (method2a . data2a) (method2b . data2b)) ;;;
;;;
////////////////////////////////////

(nutrient fluid
  (chemical-formula . r1)
  (density (constant . 1278))
  (specific-heat (constant . 4182))
  (latent-heat (constant . 2263073))
  (vaporization-temperature (constant . 284))
  (boiling-point (constant . 373))
  (volatile-fraction (constant . 1))
  (binary-diffusivity (constant . 3.05e-05))
  (thermal-conductivity (constant . 0.60000002))
  (viscosity (constant . 0.001003))
  (molecular-weight (constant . 90))
  (formation-entropy (constant . 69902.211))
  (species-phase (constant . 1))
  (lennard-jones-length (constant . 0))
  (lennard-jones-energy (constant . 0))
  (therm-exp-coeff (constant . 0))
  (degrees-of-freedom (constant . 0))
  (speed-of-sound (none . #f))
  (formation-enthalpy (constant . 0))
  (reference-temperature (constant . 298.14999))
)
```

### 11.3 FLUENT Scheme Example

This example is part of a simple scheme that was used to automate the simulation work. In general, the script below describes to FLUENT through use of the graphical user interface (GUI) what to do at the specific points in the procedure. This way FLUENT can open up a menu and change the reaction rate, iterate until converged, save the data, and then start over.

```
(cx-gui-do cx-activate-item "MenuBar*DefineMenu*Materials...")
(cx-gui-do cx-activate-item
"Materials*Frame2(Properties)*Table2(Properties)*Frame2*Frame2*PushButton2(Edi
t)")
(cx-gui-do cx-set-text-entry "Reactions*Frame1*TextEntry1(Mixture)" "mfc-
mixture")
(cx-gui-do cx-set-real-entry-list "Reactions*Frame3*Frame2(Arrhenius
Rate)*RealEntry1(Pre-Exponential Factor)" '( 5e-006))
(cx-gui-do cx-activate-item "Reactions*PanelButtons*PushButton1(OK)")
(cx-gui-do cx-set-list-selections
"Export*Frame2*Table2*Frame1*Table1*Frame5*List5(Functions to Write)" '( 32
33 34 35 36 37 38 39 40 41 42 43 44 45 46 47 48 49 50 51 52 53 54 55 62 63
64))
(cx-gui-do cx-activate-item
"Export*Frame2*Table2*Frame1*Table1*Frame5*List5(Functions to Write)")
(cx-gui-do cx-set-list-selections "Solution XY Plot*Table8*DropDownList1(X
Axis Function)" '( 0))
(cx-gui-do cx-activate-item "Solution XY Plot*Table8*DropDownList1(X Axis
Function)")
(cx-gui-do cx-set-list-selections "Solution XY Plot*Table7*DropDownList1(Y
Axis Function)" '( 5))
(cx-gui-do cx-activate-item "Solution XY Plot*Table7*DropDownList1(Y Axis
Function)")
(cx-gui-do cx-activate-item
"Materials*PanelButtons*PushButton1(Change/Create)")
(cx-gui-do cx-activate-item "Materials*PanelButtons*PushButton1(Close)")
(cx-gui-do cx-activate-item "MenuBar*SolveMenu*Iterate...")
(cx-gui-do cx-activate-item "Iterate*PanelButtons*PushButton1(OK)")
(cx-gui-do cx-set-list-selections
"Export*Frame2*Table2*Frame1*Table1*Frame5*List5(Functions to Write)" '( 32
33 34 35 36 37 38 39 40 41 42 43 44 45 46 47 48 49 50 51 52 53 54 55 62 63
64))
(cx-gui-do cx-activate-item
"Export*Frame2*Table2*Frame1*Table1*Frame5*List5(Functions to Write)")
(cx-gui-do cx-set-list-selections "Solution XY Plot*Table8*DropDownList1(X
Axis Function)" '( 0))
(cx-gui-do cx-activate-item "Solution XY Plot*Table8*DropDownList1(X Axis
Function)")
(cx-gui-do cx-set-list-selections "Solution XY Plot*Table7*DropDownList1(Y
Axis Function)" '( 5))
(cx-gui-do cx-activate-item "Solution XY Plot*Table7*DropDownList1(Y Axis
Function)")
(cx-gui-do cx-activate-item "MenuBar*WriteSubMenu*Case & Data...")
(cx-gui-do cx-set-text-entry "Select File*Text" "oxi_lxcat_a5e-6")
(cx-gui-do cx-activate-item "Select File*OK")
```

### 11.3.1 Calculations

#### Dimensions

#### Surface to Volume ratio

Normally the surface to volume ratio for electrodes is provided from the manufacturer, but since this information was not provided for the electrodes used in the experiments in Case 1. The aim is to find a value for the surface to volume ratio, which can be written as:

$$\text{I} \quad \text{Surface / Volume} = \frac{A}{V}$$

Since it is not possible to find the surface area of the electrode (A), other more measurable properties must be used. It was therefore calculated from the porosity of the electrode and the dimension of the wires that were used to create the electrodes.

First it was assumed that the whole electrode was produced by one thin graphite wire, and the wire is assumed to not be touching at any place of significant area. The surface area of the electrode can therefore be found from the following equation:

$$A = \text{surface\_area} = \text{length} * 2\pi = L * \pi d$$

And can be rewritten as

$$\text{II} \quad L = \frac{A}{\pi d}$$

The porosity of the electrode is defined as 1 minus the free volume. The free volume can be found from the (total weight of the electrode / volume)/density of solid graphite. The porosity is therefore found by:

$$\text{III} \quad P = 1 - \frac{m/v}{\rho_{\text{graphite}}}$$

Now, the mass of the graphite felt can be found two different ways which will be used to find the surface to volume ratio.

$$\text{IV} \quad m_{\text{electrode}} = V_{\text{electrode}} * \rho_{\text{graphite}} * (1 - P)$$

$$\text{V} \quad m_{\text{electrode}} = V_{\text{wires}} * \rho_{\text{graphite}} = L_{\text{wire}} * \frac{\pi d^2}{4} * \rho_{\text{graphite}}$$

By inserting II in V, it is possible to write the mass in a third way, which then can be simplified further:

$$\text{VI} \quad m_{\text{electrode}} = L_{\text{wire}} * \frac{\pi d^2}{4} * \rho_{\text{graphite}} = \frac{A}{\pi d} * \frac{\pi d^2}{4} * \rho_{\text{graphite}} = \frac{Ad}{4} * \rho_{\text{graphite}}$$

And by setting equation VI equal to equation IV, it is possible to find a new relationship for the surface to volume ratio:

$$\text{VII} \quad \frac{Ad}{4} * \rho_{\text{graphite}} = V_{\text{electrode}} * \rho_{\text{graphite}} * (1 - P)$$

$$\frac{A}{V_{\text{electrode}}} = \frac{4(1 - P)}{d}$$

When measuring the graphite felt, it is found to be 0.6g, with a projected surface area of 11.94cm<sup>2</sup> and a thickness of 6mm. The density of graphite is found to be between 2.09-2.23 g/cm<sup>2</sup> ~ 2.2g/cm<sup>2</sup>. By using equation III this gives a porosity of:

$$\text{VIII} \quad P = 1 - \frac{m/v}{\rho_{\text{graphite}}} = 1 - \frac{0.6g / (11.94\text{cm}^2 * 0.6\text{cm})}{2.2g / \text{cm}^3} = 0.96$$

By using equation VII, the Surface / Volume ratio is found to be:

$$\text{IX} \quad \frac{A}{V_{\text{electrode}}} = \frac{4(1 - P)}{d} = \frac{4(1 - 0.96)}{15 * 10^{-6}} = \underline{\underline{10666}}$$